Rhodium and Iridium β-Diiminate Complexes – Olefin Hydrogenation Step by Step

Peter H. M. Budzelaar,*[a] Nicolle N. P. Moonen,[a] René de Gelder,[a] Jan M. M. Smits,[a] and Anton W. Gal[a]

Keywords: Hydrogenation / Isomerization / Rhodium / Iridium / Hydrides

The bulky β-diiminate ligands $[(2,6\text{-}C_6H_3X_2)NC(Me)CHC(Me)N(2,6\text{-}C_6H_3X_2)]^-$ (X = Me, L_{Me}; X = Cl, L_{Cl}) have been found to be effective in stabilizing low coordination numbers (CN) in Rh and Ir complexes. The 14-*e* complex L_{Me}Rh(COE) (COE = cyclooctene) has a three-coordinate T-shaped Rh environment and is nonagostic. Coordinative unsaturation is avoided by incorporation of a small ligand (e.g. N_2, MeCN, olefins), by the intramolecular coordination of a chlorine atom in L_{Cl}Rh(COE), or by an agostic interaction in L_{Me}Rh(norbornene). In solution at room temperature, L_{Me}Rh(COE) undergoes rapid isomerization according to the allyl hydride mechanism; the corresponding 2,3-dimethylbutene complex actually prefers the allyl hydride structure. Rhodium(I) complexes of L_{Me} and L_{Cl} catalyze olefin hydrogenation; hydrogenation of 2,3-dimethylbutene has been shown to be preceded by isomerization. The shielding properties of the bulky β-diiminate ligands allow direct observation of a number of reactive intermediates or their iridium analogues, including an olefin–dihydrogen complex (with Rh) and an olefin dihydride (with Ir). These observations, together with calculations on simple model systems, provide us with snapshots of a plausible hydrogenation cycle. Remarkably, hydrogenation according to this cycle appears to follow a 14-*e*/16-*e* path, in contrast to the more usual 16-*e*/18-*e* paths.

Introduction

Coordinatively unsaturated species are key intermediates in most catalytic cycles. Because of their high reactivity, they can rarely be isolated or even observed directly. Therefore, it is necessary to rely on indirect information (e.g. from trapping experiments or kinetics) to deduce the characteristic properties of such species. Obviously, isolable unsaturated species are of interest because they present an opportunity to study the reactivity of key intermediates *directly*.

We recently found that β-diiminate ligands can be effective in stabilizing low coordination numbers. With early transition metals, this has led to the isolation of stable four-coordinate Ti^{III} and V^{III} dialkyls.[1] In our recent work on late transition metals, we isolated a stable (but still highly reactive) 14-*e* rhodium(I) olefin complex.[2] We now describe the synthesis, characterization, and reactivity of Rh and Ir complexes of two bulky β-diiminate ligands, L_{Me} and L_{Cl}. The Rh complexes have proved to be active in olefin isomerization and hydrogenation. More importantly, we have found that the shielding properties of these ligands allow the direct observation of a number of species that can be envisaged as intermediates in isomerization and hydrogenation cycles, including a rhodium olefin–dihydrogen complex and an iridium olefin–dihydride complex. As an aid to interpretation of the results, B3LYP calculations have been performed on complexes of the model ligand L.

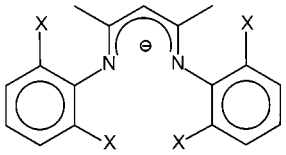

L_{Me} X = Me
L_{Cl} X = Cl

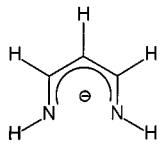

L

Other examples of coordinatively unsaturated species stabilized by bulky ligands have been reported. Some relevant examples are three-coordinate 14-*e* rhodium(I) complexes L_2RhX (L = bulky phosphane)[3] and the remarkable 14-*e* iridium dihydride complex $[P(t\text{Bu})_2Ph]_2IrH_2^+$ described by Caulton.[4] However, we are not aware of any example of a 14-*e* Rh or Ir complex bearing a labile and easily displaceable olefin ligand.

Results and Discussion

Ethene and Cyclooctadiene Complexes

The β-diimine ligand $L_{Me}H$ may easily be prepared by condensation of 2,4-pentanedione and 2,6-dimethylaniline. Reaction with $LiN(i\text{Pr})_2$ in THF produces the lithium salt L_{Me}Li(THF), which is obtained from hexane in the form of off-white crystals. The ligand $L_{Cl}H$ and its lithium salt may be prepared similarly; L_{Cl}Li(THF) forms large yellow crystals from toluene/hexane, which slowly turn reddish on exposure to light.

Reaction of L_RLi(THF) (L_R = L_{Me} or L_{Cl}) with $[Rh(COD)Cl]_2$ (COD = 1,5-cyclooctadiene) produces the

[a] Department of Inorganic Chemistry, University of Nijmegen, Toernooiveld 1, NL-6525 ED Nijmegen, The Netherlands
E-mail: budz@sci.kun.nl

  1434–1948/00/0404–0753 $ 17.50+.50/0

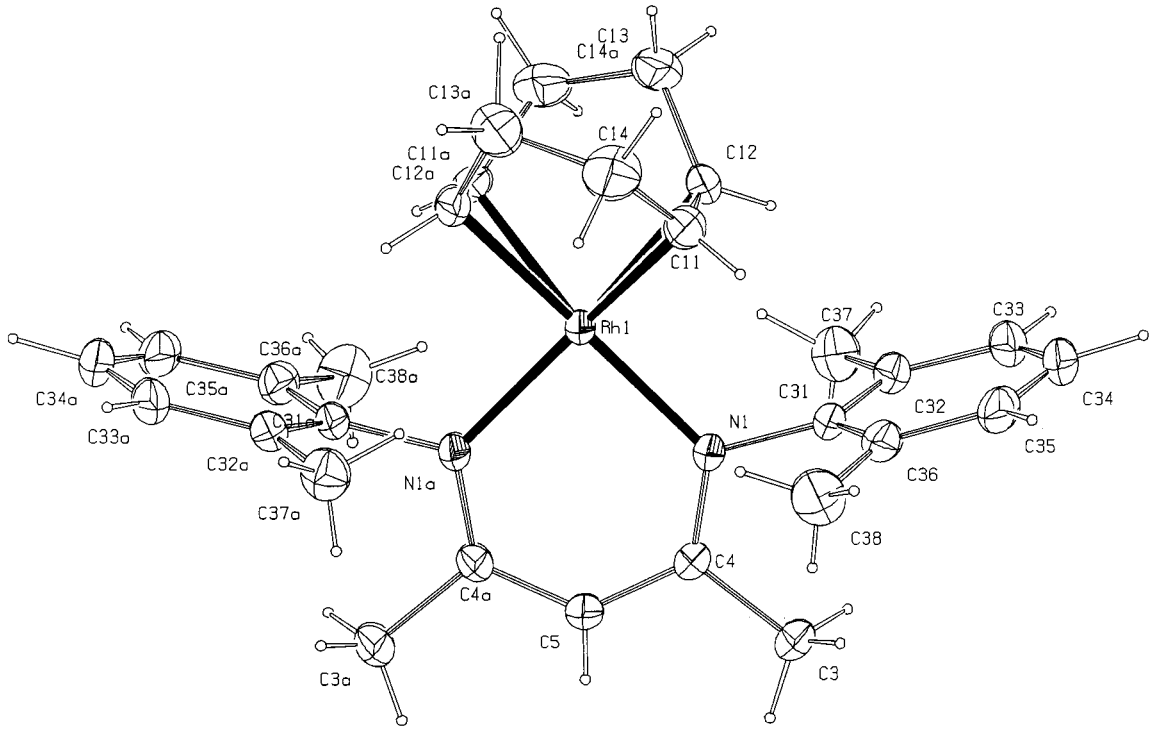

Figure 1. X-ray structure (30% ellipsoids) of $L_{Me}Rh(COD)$; atoms labelled *a* are related to original atoms by a twofold axis through Rh1 and C5; selected bond lengths (Å): Rh1–C11 2.138(2), Rh1–C12 2.169(2), Rh1–N1 2.0953(15)

very stable 16-*e* complexes $L_RRh(COD)$; ethene complexes $L_RRh(C_2H_4)_2$ can be obtained in a similar manner from $[Rh(C_2H_4)_2Cl]_2$. The X-ray structures of $L_{Me}Rh(COD)$ (Figure 1) and $L_{Me}Rh(C_2H_4)_2$ (Figure 2, A) show the expected square-planar coordination geometries. The bis(ethene) complex has perpendicular ethene ligands, which are tilted slightly out of the coordination plane in opposite directions. Distortions of this kind have been observed for *cis*-bis(ethene) complexes containing a chiral ligand; theoretical studies indicate that such structures are relatively easily deformed.[5]

The optimized structure of model complex $LRh(C_2H_4)_2$ shows a regular four-coordinate Rh atom. The calculated Rh–N distance (2.03 Å) is shorter than those observed for $L_{Me}Rh(C_2H_4)_2$ (av. 2.09 Å) and $L_{Me}Rh(COD)$ (av. 2.10 Å), while the Rh–C distances are longer (av. 2.28 Å vs. 2.15 Å). It is possible that the main cause of these discrepancies lies in the choice of model system: the aryl substituents on the L_{Me} ligand will weaken the N–Rh coordination and hence strengthen the Rh–olefin bond relative to the situation in the unsubstituted model ligand L. This means that we can also expect an underestimation of the calculated interaction strength of the LRh fragment with other added ligands.

In the calculated structure of $LRh(C_2H_4)_2$, the centers of the olefin ligands lie exactly in the coordination plane. If, however, the N–Rh–olefin angles are constrained to the value of 94° observed in the X-ray structure of $L_{Me}Rh(C_2H_4)_2$, a nonplanar structure is obtained. This suggests that the nonplanarity in the L_{Me} complex is caused by repulsion between the ethene hydrogens, as a result of the steric demand of the ligand aryl groups. A space-filling model of $L_{Me}Rh(C_2H_4)_2$ indeed shows interlocking of the ethene hydrogens and close contacts between the olefins and the aryl groups (Figure 2, B). Accordingly, the NMR spectra show that ethene rotation is blocked at room temperature. Crowded [bis(oxazolinyl)methanate]Rh(ethene)$_2$ complexes also show hindered rotation,[5] but in relatively open bis(ethene) complexes of β-diketonates and β-ketoiminates ethene rotation is usually fast at room temperature.[6]

Cyclooctene Complexes

The above results suggested that two molecules of a bulkier olefin, e.g. a *cis*-disubstituted olefin, would not fit into the cleft between the aryl groups: the substituents at the double bond of one olefin would interfere either with the arene ring or with the other olefin ligand. Indeed, reaction of $L_{Me}Li(THF)$ with $[Rh(COE)_2Cl]_2$ (COE = cyclooctene) was found to produce the deep-purple *mono*-olefin complex $L_{Me}Rh(COE)$ in moderate yield (70%). This complex proved to be extremely air-sensitive, but otherwise stable at room temperature. The X-ray structure[2] showed the molecule to be disordered over a twofold symmetry axis; this disorder could be refined satisfactorily (Figure 3). The coordination geometry about Rh is roughly T-shaped, but the olefin is shifted somewhat towards the center of the open cleft (N–Rh–olefin = 112°). Remarkably, there are no short agostic interactions.

Unfortunately, the disorder prevents us from obtaining individual distances for the two types of Rh–N bond. In the model compound $LRh(C_2H_4)$, we see a shortening of the Rh–C and Rh–N distances (by 0.07 and 0.04 Å, respectively) relative to those in the bis(ethene) complex. Accord-

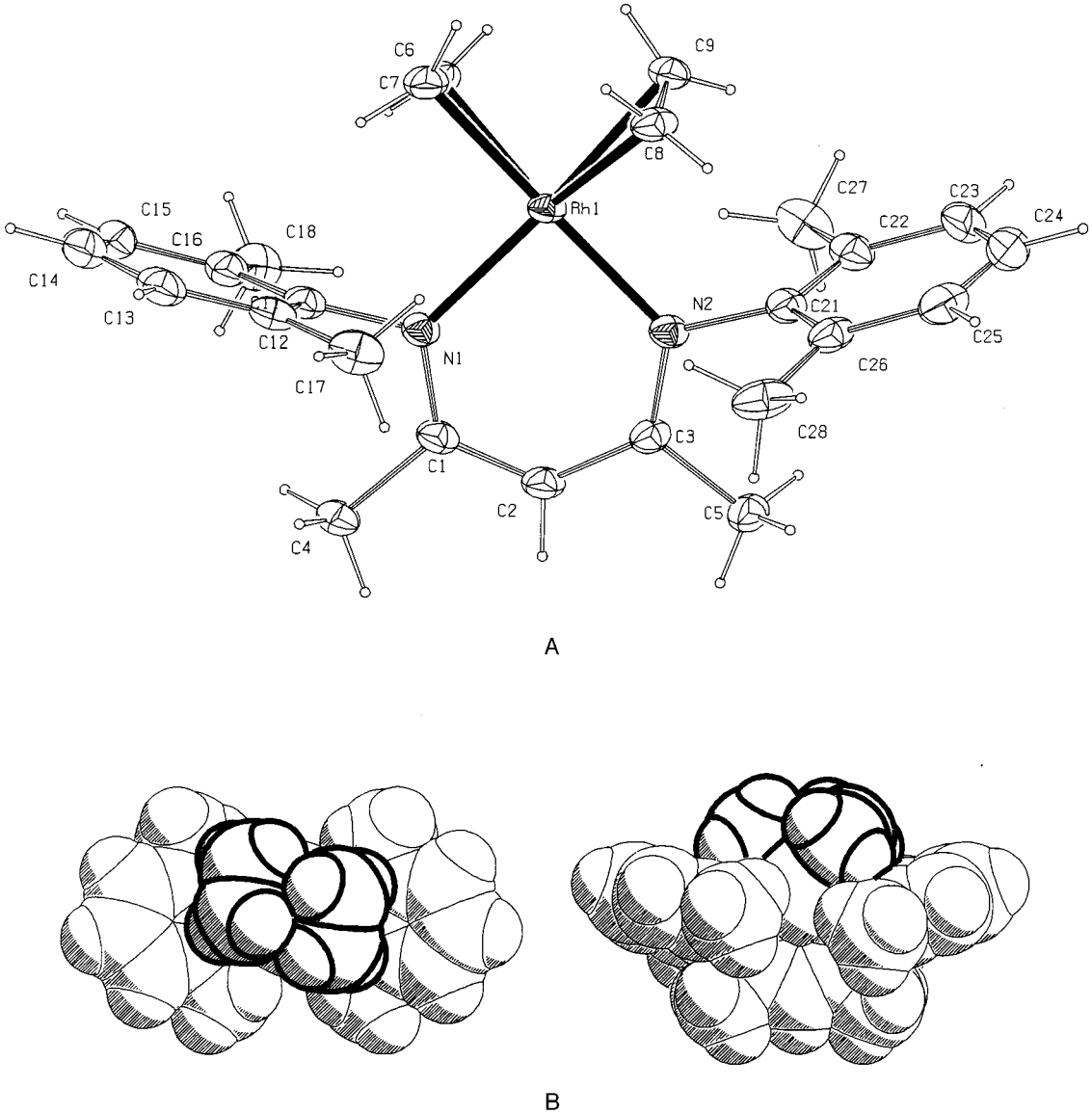

Figure 2. A: X-ray structure (30% ellipsoids) of $L_{Me}Rh(C_2H_4)_2$; B: space-filling model, outline of the ethene ligands emphasized; selected bond lengths (Å) and angles (°): Rh1–C6 2.131(4), Rh1–C7 2.155(4), Rh1–C8 2.133(4), Rh1–C9 2.160(4), Rh1–N1 2.093(3), Rh1–N2 2.086(3), C6–C7 1.390(7), C8–C9 1.367(7); N1–Rh1–N2 89.11(12)

ing to the X-ray data, the Rh–C bonds in $L_{Me}Rh(COE)$ are about 0.08 Å shorter than those in $L_{Me}Rh(C_2H_4)_2$ and $L_{Me}Rh(COD)$, while the Rh–N bonds are about 0.13 Å shorter. However, the X-ray bond lengths obtained for the COE complex must be treated with caution since the two alternative Rh positions, which differ by as much as 0.1 Å, could not be resolved in the structure determination. The N–Rh–olefin angle of 94° calculated for $LRh(C_2H_4)$ is larger than the 88° calculated for $LRh(C_2H_4)_2$, but much smaller than the value of 112° observed in $L_{Me}Rh(COE)$. The calculated barrier associated with ethene transfer between the two vacant sites of $LRh(C_2H_4)$ is only 11 kcal/mol. Thus, we attribute the distortion of $L_{Me}Rh(COE)$ towards a trigonal geometry to the steric demand of the aryl groups, coupled with a low barrier for movement of the olefin.[7]

Solution NMR data at –60 °C[8] are consistent with the solid-state structure, showing discrete resonances for the diiminate halves *cis* and *trans* to the olefin. At room temperature, however, the L_{Me} ligand has effective C_{2v} symmetry, and only two broadened resonances are observed for the cyclooctene ligand in the ^1H spectrum, corresponding to 6 and 8 protons, respectively. We attribute this dynamic behavior to rapid equilibration between olefin and allyl hydride isomers.[9] This scrambles the COE hydrogens in two groups: (i) all *endo* hydrogens (6 H) and (ii) all *exo* hydrogens together with the vinylic hydrogens (8 H). Any intermolecular process would result in complete scrambling of all 14 COE hydrogens.

Owing to the complicated nature of the spectrum, we could not extract the activation energy, but the temperature region in which coalescence is observed (–50 to –20 °C) in-

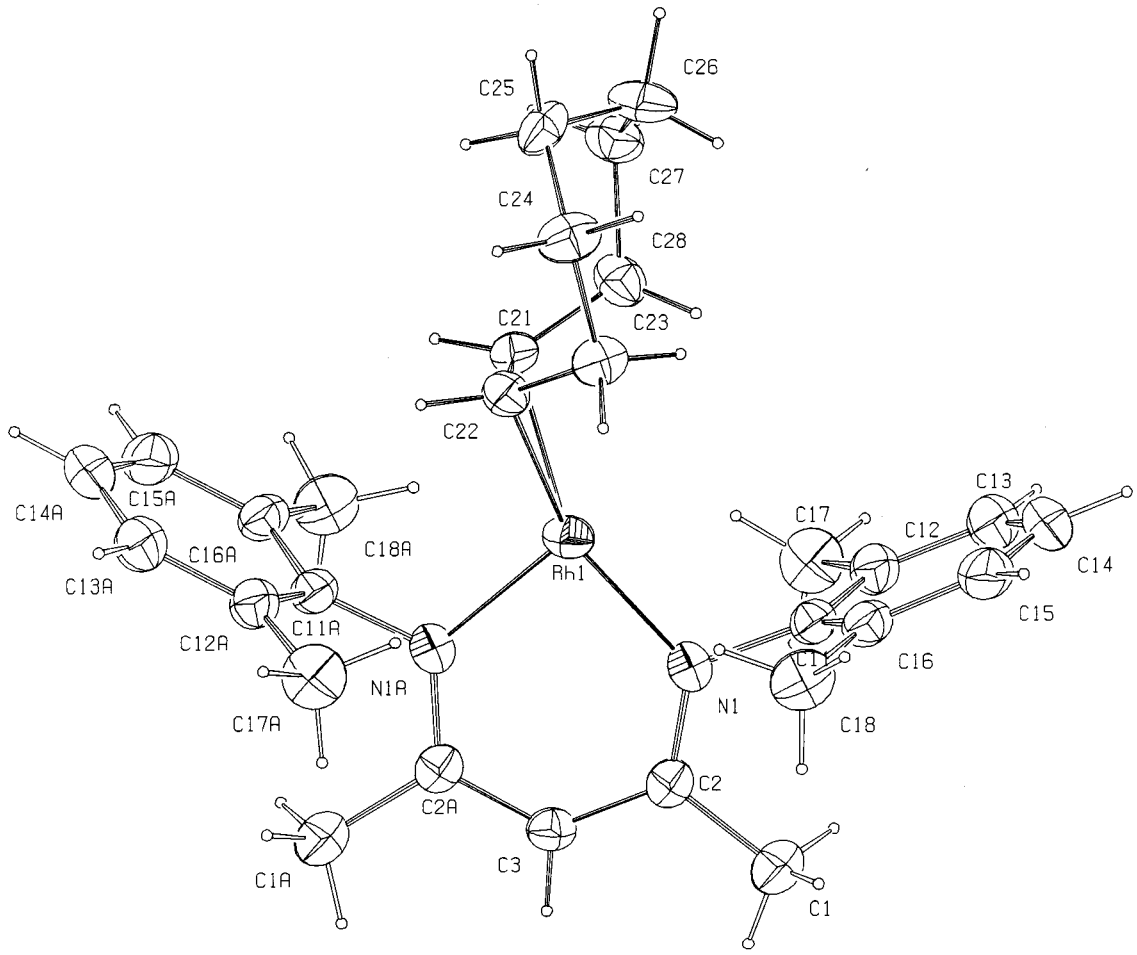

Figure 3. X-ray structure (30% ellipsoids) of $L_{Me}Rh(COE)$ (see ref.[2]); only one of the two cyçlooctene images is shown; atoms labelled *a* are related to original atoms by a twofold axis through Rh1 and C3; selected bond lengths (Å) and angles (°): Rh1–N1 1.955(2), Rh1–C21 2.072(5), Rh1–C22 2.066(6), C21–C22 1.398(7); N1–Rh1–N1a 91.3(1)

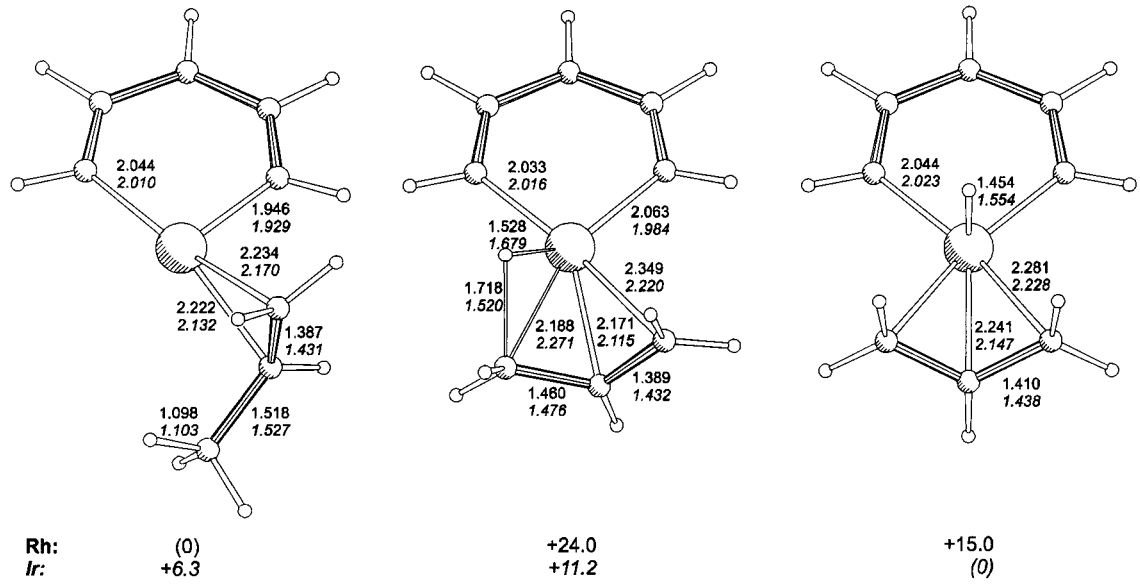

Figure 4. Calculated structures and energies (kcal/mol) for olefin–allyl hydride isomerization of LRh(propene); energies and parameters for the Ir analogs given in italics

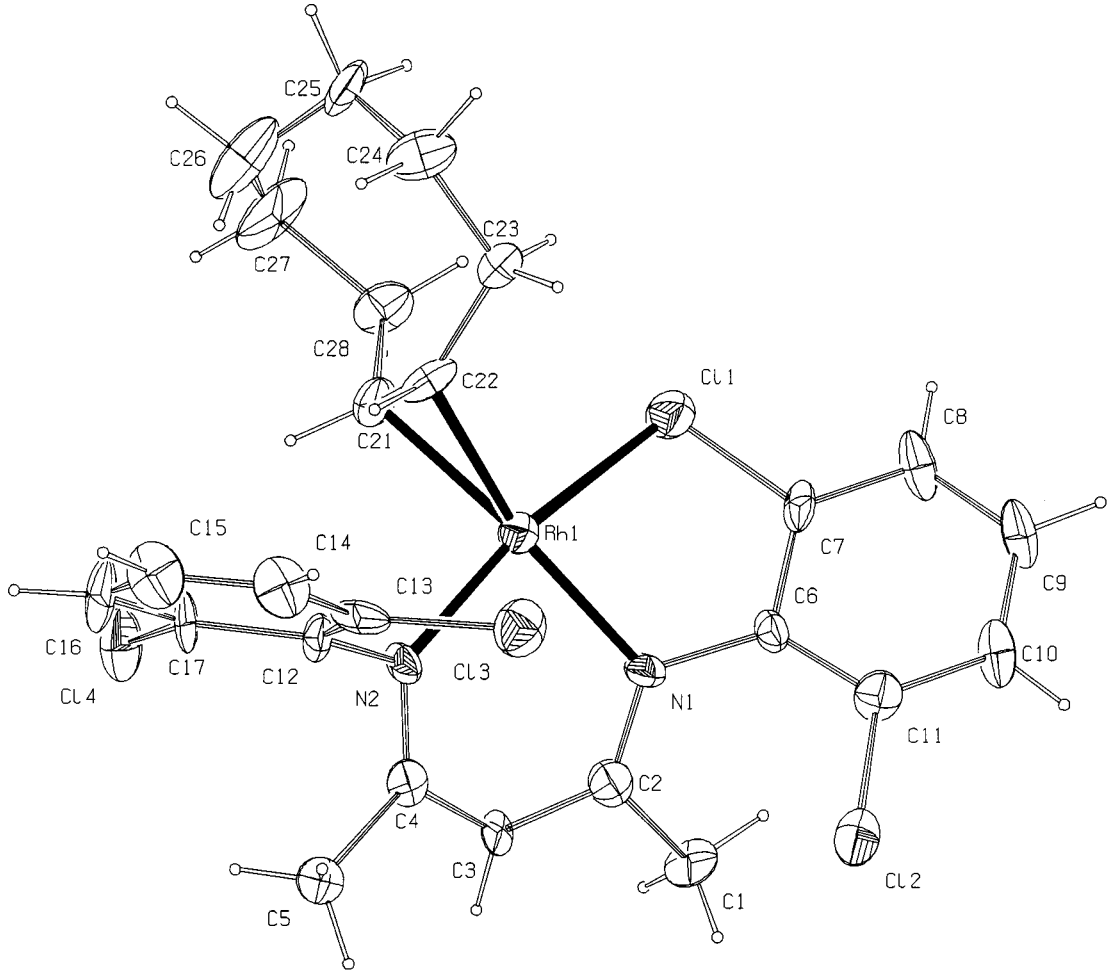

Figure 5. A: X-ray structure (30% ellipsoids) of $L_{Cl}Rh(COE)$; only one of the two independent molecules is shown; B: projection along N1–N2, illustrating the displacement of Rh out of the diiminate plane; selected bond lengths (Å) and angles (°): Rh1–C21 2.088(16), Rh1–C22 2.128(16), Rh1–N1 2.040(12), Rh1–N2 1.996(13), Rh1–Cl1 2.376(5), C21–C22 1.37(2), Rh2–C51 2.155(16), Rh2–C52 2.106(16), Rh2–N31 2.062(14), Rh2–N32 2.048(15), Rh2–Cl31 2.365(5), C51–C52 1.39(2); N1–Rh1–N2 89.2(5), N1–Rh1–Cl1 80.0(4), N31–Rh2–N3 291.2(6), N31–Rh2–Cl31 80.3(4)

dicates a barrier of ca. 12 kcal/mol. B3LYP calculations confirm that the olefin complex LRh(propene) is more stable than the isomeric LRh(allyl)(H),[10] but the calculated energy difference is rather large (15 kcal/mol), and the calculated barrier of 24 kcal/mol is much larger than the experimental value for $L_{Me}Rh(COE)$. The difference of 12 kcal/mol between calculated and observed barriers might be attributable to deficiencies in the theoretical methods used[11] and/or to an absence of steric effects in the model system.[12] Figure 4 shows the calculated structures for the

two isomers and the transition state. The allyl hydride complex has a square-pyramidal structure, with the hydride occupying the apical position and the two outer allyl carbons in equatorial positions.

Reaction of $L_{Me}Li(THF)$ with $[Ir(COE)_2Cl]_2$ proceeded more slowly than in the Rh case, and the product was found to be unstable at room temperature (vide infra). Therefore, only a low yield (ca. 10%) of orange "$L_{Me}Ir(COE)$" could be obtained from this reaction. The ^1H- and ^{13}C-NMR spectra of this complex unambiguously establish a static allyl hydride structure $L_{Me}Ir(H)$(cyclooctenyl) ($\delta_H = -46.2$).[13] Repeated attempts to crystallize the product resulted only in poor crystals, which nevertheless allowed the connectivity to be established; this connectivity was consistent with the calculated structure shown in Figure 4. B3LYP calculations indicate that on going from Rh to Ir the relative stabilities of the olefin and allyl hydride isomers are indeed inverted (Figure 4).[14]

In the hope of obtaining a 14-*e* complex with a disorder-free structure, we also prepared red $L_{Cl}Rh(COE)$. The X-ray structure shows coordination of one of the chlorine atoms of the diiminate ligand to the metal (Figure 5). The rhodium atom is displaced out of the diiminate plane to allow close approach to the chlorine. In solution, this complex shows the same allyl hydride dynamic behavior as $L_{Me}Rh(COE)$, although the coalescence temperature is slightly higher. At –60 °C, the allyl hydride exchange is completely frozen out, but exchange of the two chlorine atoms of the chelating dichlorophenyl group remains rapid. The facile dissociation of the Rh–Cl bond in solution, as observed by NMR, does not imply that this is an intrinsically weak interaction. It merely shows that the diiminate ligand deformation needed to achieve Rh–Cl coordination requires nearly as much energy as is gained through formation of the coordination bond.

2,3-Dimethyl-2-butene Complex

When a solution of $L_{Me}Rh(COE)$ in 2,3-dimethyl-2-butene is stirred under hydrogen for a few minutes, all cyclooctene is lost as cyclooctane. After removal of the volatiles, the ^1H-NMR spectrum of the residue in $[D_8]$THF or C_6D_{12} shows strongly broadened signals attributable to a 2,3-dimethylbutene complex.[15] Apparently, *all* olefinic hydrogens in this complex are exchanging on the NMR timescale. Cooling of a $[D_8]$THF solution to –30 °C results in decoalescence of the diiminate 3-H signal into two signals of relative intensity 4:1 and considerable sharpening of the rest of the spectrum. At this temperature, the major component of the mixture (corresponding to the largest 3-H signal) gives rise to fairly sharp isopropyl group resonances (δ = 1.85 and 1.24) and a broad resonance at $\delta = -2.45$, which integrates for approximately 5 protons. Further cooling results in broadening of the resonance at $\delta = -2.45$, but at –60 °C (just above the melting point of THF) the static limit still has not been reached. Because of the multitude of peaks due to the major component and the oxidation product,[15] we cannot assign any peaks due to the minor component in the region δ = 0–2.5. However, below –40 °C, a clear hydride signal is seen at $\delta = -12$ with the appropriate intensity for 1 H of the minor component. In the ^{13}C spectrum, all peaks due to the major component and some peaks due to the minor component can be assigned.

Scheme 1 illustrates the interconversion of the isomers that can be formed from $L_{Me}Rh$(2,3-dimethyl-2-butene). The major component in the low-temperature spectrum must correspond to allyl hydride isomer **E** in equilibrium with olefin complex **D**. The observed average shift of $\delta = -2.45$ for the five protons not belonging to the isopropyl group is compatible with structure **E** but not with **D**. Thus, in contrast to cyclooctene, the equilibrium for this olefin lies on the side of the allyl hydride isomer. The minor component, which gives rise to a hydride resonance below –40 °C, must therefore be allyl hydride isomer **B**. In the olefin complexes **A**, **C**, and **D**, at least one of the substituents at the double bond points towards the diiminate aryl groups. It seems likely that steric repulsion makes the olefin complexes less stable than the allyl hydride isomers **B** and **E**.

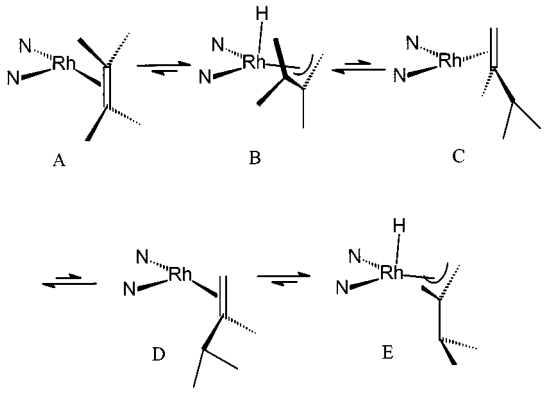

Scheme 1. Proposed mechanism for the dynamic behavior of "$L_{Me}Rh$(2,3-dimethyl-2-butene)"

Norbornene Complex

The facile allyl hydride isomerization of cyclooctene and 2,3-dimethylbutene complexes made us wonder whether olefin complexes not containing any available allylic hydrogens would be prone to a similar C–H activation of more remote C–H bonds. Therefore, we tried to prepare a norbornene (NBE) analog of $L_{Me}Rh(COE)$ starting from $[Rh(NBE)_2Cl]_2$. This reaction invariably produced a very dark-colored mixture of complexes. ^1H-NMR showed the presence of a small amount (ca. 10%) of a compound giving signals at $\delta = -10.2$ (dd) and $\delta = -1.2$ (d), but we were not successful in isolating it from the mixture. However, treatment of $L_{Me}Rh(COE)$ with a threefold excess of NBE in hexane resulted in clean formation of the same compound in the form of red-brown crystals. The X-ray structure (Figure 6) shows that it is indeed a close analog of $L_{Me}Rh(COE)$, with a similarly distorted T-shaped coordination geometry. In this case, however, there is a clear agostic interaction with an Rh–H distance of less than 2 Å[16] [RhC = 2.531(4) Å]. This pronounced agostic interac-

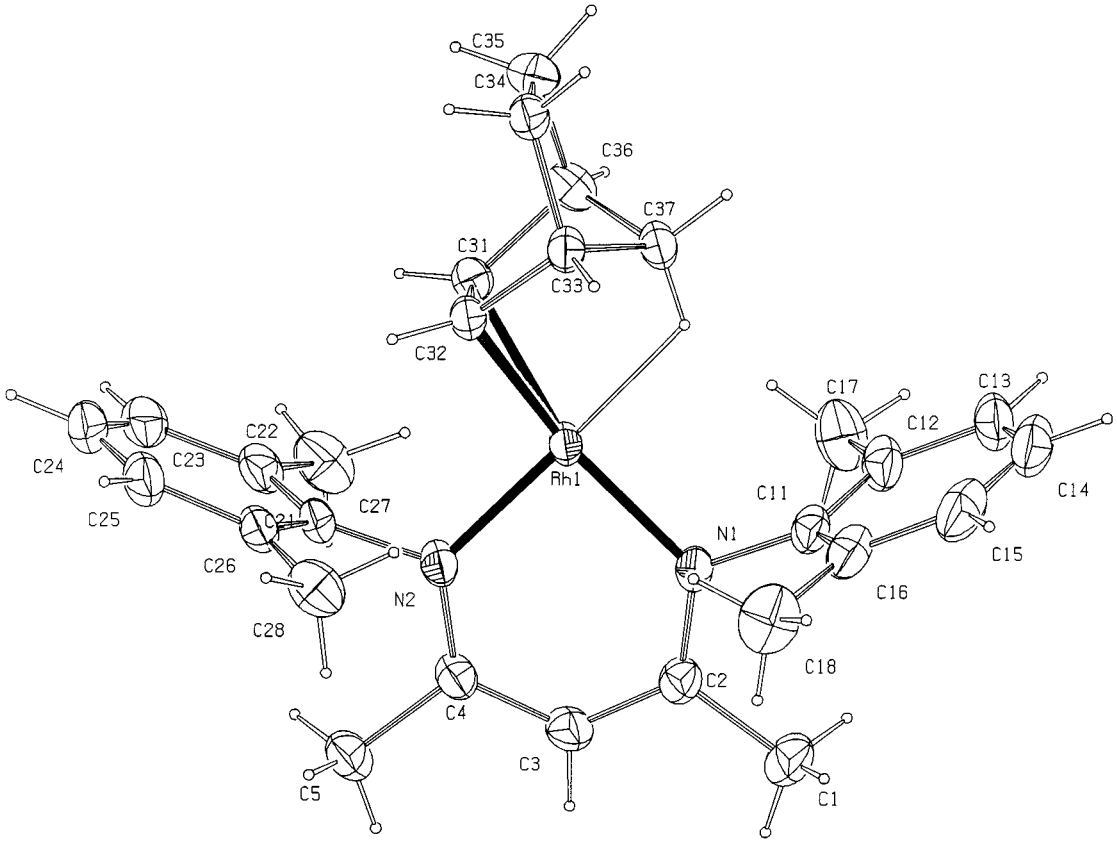

Figure 6. X-ray structure (30% ellipsoids) of L_{Me}Rh(NBE); selected bond lengths (Å) and angles (°): Rh1–C31 2.115(4), Rh1–C32 2.095(4), Rh1–C37 2.531(4), Rh1–N1 2.021(3), Rh1–N2 1.985(3), C31–C32 1.395(6); N1–Rh1–N2 91.12(13)

tion accounts for the unusual high-field shift (δ = –10.2) of the bridge proton, which would more typically be associated with metal-bound hydrides. The alternative formulation as a cyclometallated olefin complex can be ruled out as the RhC distance is much too great for a single bond. Moreover, the methylene carbon is seen to be coupled to both hydrogens (J = 108 and 141 Hz), but shows no measurable coupling to Rh. Close approach of an NBE methylene hydrogen to a metal has also been observed in (dien)Cu(NBE)$^+$ [CuC = 2.78(1) Å, CuH = 2.01(15) Å],[17] but in the three other NBE complexes for which X-ray structures have been reported the distances between the metal and the methylene bridges are much larger: [(*t*Bu)$_2$P(CH$_2$)$_2$P(*t*Bu)$_2$]Pt(NBE) (PtC = 3.18 Å, PtH = 2.75 Å),[18] Pt(NBE)$_3$ (PtC = 3.20/3.13/3.16 Å, PtH = 2.65/2.80/3.01 Å),[19] and a dicopper complex (CuC = 2.96/2.97 Å, CuH = 2.50/2.51 Å).[20]

The observation of a pronounced agostic interaction in L_{Me}Rh(NBE) provides little information concerning the *strength* of this interaction. In fact, the NBE ligand appears to be predisposed towards such an agostic interaction; in the absence of any (repulsive or attractive) Rh–H forces, one would expect a structure very similar to the one observed. One observation that disfavours a strong agostic bond is the fact that such a bond is not observed at all in L_{Me}Rh(COE), despite the fact that only a modest deformation of either the COE or the diiminate ligand would be required to obtain a short Rh–H contact.

In order to clarify this point, we carried out calculations on LRh(NBE). These reproduced most of the features of the X-ray structure of L_{Me}Rh(NBE), although the shortening of Rh-C distances relative to those in the corresponding bis(ethene) complex was overestimated (calcd. 0.09 Å, obsd. 0.04 Å), while that of the Rh-N distances was underestimated (calcd. 0.02 Å, obsd. 0.09 Å). The agostic interaction is somewhat weaker in the calculated structure [RhH = 2.20 Å, RhC = 2.77 Å vs. 2.531(4) Å]; the agostic C–H bond is only slightly elongated (1.108 Å vs. 1.094 Å for the nonagostic bond). The angles about the methylene carbon are normal and there is no significant tilting of the NBE ligand towards the Rh atom. The calculated structure of LRh(NBE) is closer to T-shaped (N−Rh−olefin = 96°) than that observed for L_{Me}Rh(NBE) (N−Rh−olefin = 102°); again, this may probably be attributed to the absence of steric constraints (vide supra) in the model. Fixing the N−Rh−olefin angle at 102° in the calculations costs only 0.7 kcal/mol and results in a slightly longer Rh−olefin bond (2.100 vs. 2.075 Å) and a more pronounced agostic interaction (RhC = 2.72 Å, RhH = 2.13 Å, C−H = 1.110 and 1.095 Å). Nevertheless, there are still no indications that the agostic interaction corresponds to a strong bond.[21]

L_{Me}Rh(NBE) was found to be much less sensitive to air than L_{Me}Rh(COE): a solution in THF had to be shaken in air for several minutes to effect complete oxidation, which was accompanied by liberation of NBE and formation of uncharacterizable rhodium complexes. We assume that the

relative inertness of the NBE complex reflects the inability (for steric reasons) of the NBE ligand to allow access to the fourth coordination site through rotation, and is not related to a large direct agostic bonding energy.

Complexes with Added Ligands

Because of its vacant coordination site, $L_{Me}Rh(COE)$ can be expected to be reactive towards added donor ligands. Indeed, reaction with excess acetonitrile gives yellow $L_{Me}Rh(COE)(MeCN)$, which has the expected square-planar structure (Figure 7). In THF or cyclohexane solution, $L_{Me}Rh(COE)$ reacts with dinitrogen to form brown $L_{Me}Rh(COE)(N_2)$ ($\tilde{\nu}_{NN}$ = 2172 cm^{-1}), from which the N_2 is lost in vacuo. NMR data indicate that the dinitrogen complex also has the expected static square-planar structure. In view of the weakness of the N_2 complexation in $L_{Me}Rh(COE)(N_2)$, it is hardly surprising that agostic $L_{Me}Rh(NBE)$ and 4-coordinate $L_{Cl}Rh(COE)$ do not react with N_2. Reaction of $L_{Me}Rh(COE)$ with excess 1-hexene results in a brown solution, presumably containing $L_{Me}Rh(COE)(hexene)$. On evacuation, this complex loses olefin to give a mixture of $L_{Me}Rh(COE)$ and $L_{Me}Rh(hexene)$ (ca. 4:1 by NMR).

No reaction was observed with TMEDA. NMR spectra of $L_{Me}Rh(COE)$ in cyclohexane, benzene, toluene, and THF are virtually identical, showing the same olefin–allyl hydride dynamic behaviour. Thus, it is evident that THF does not coordinate either.[8] Steric factors may be involved, or it may be that interaction with pure σ-donors such as ethers and amines is weak. Table 1 lists the calculated binding energies for various simple donor molecules at the $LRh(C_2H_4)$ and $LIr(C_2H_4)$ fragments. Bonds to Ir are consistently stronger than those to Rh; for both metals, the order is $H_2 < C_2H_4 \approx$ MeCN $\approx Me_2O \approx N_2 <$ CO. Ligands allowing strong back-donation, such as H_2 and CO, show the largest differences

Table 1. Calculated ligand binding energies of $LRh(C_2H_4)$ and $LIr(C_2H_4)$ fragments [kcal/mol]

Ligand	$LRh(C_2H_4)$	$LIr(C_2H_4)$
CO	40.6	71.2
N_2	30.5	48.2
Me_2O	29.9	35.3
MeCN	28.4	44.7
C_2H_4	24.4	46.3
H_2	11.1	33.2

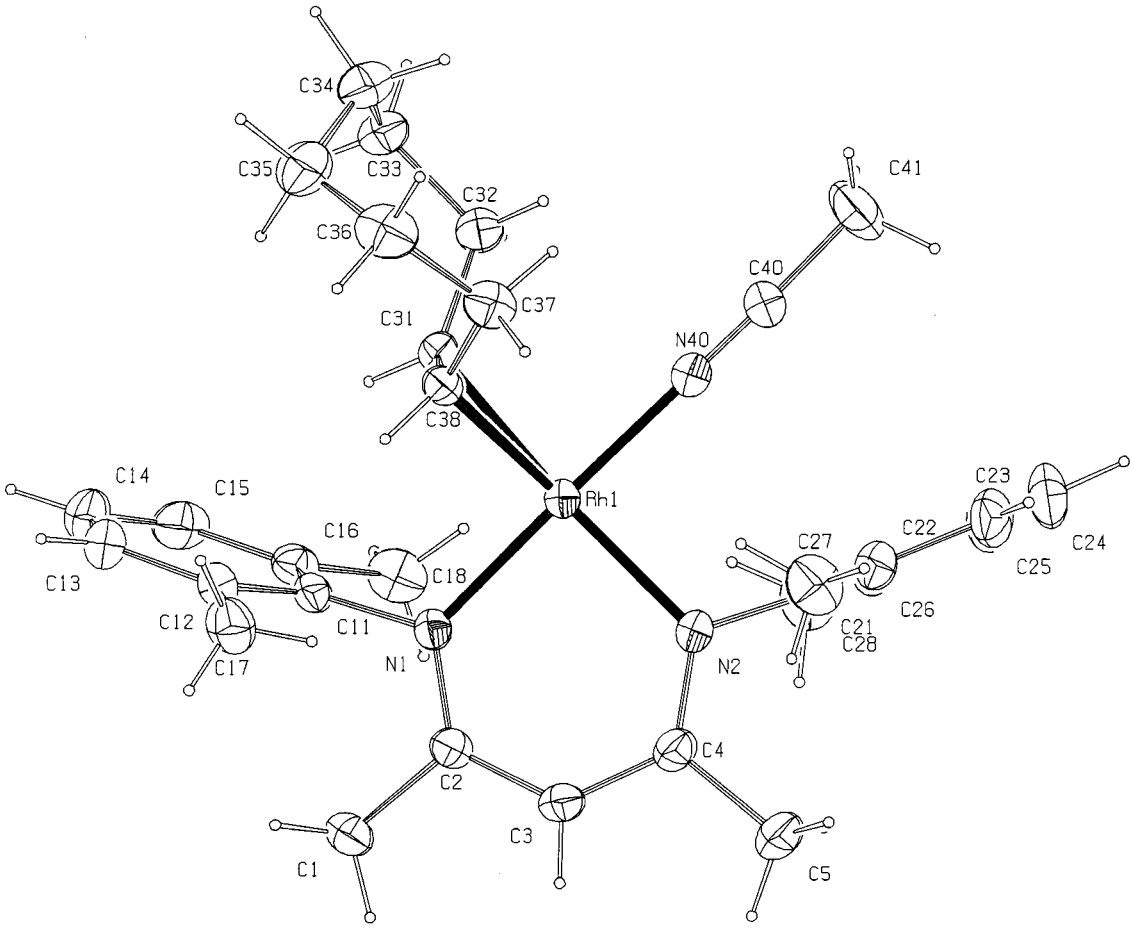

Figure 7. X-ray structure (30% ellipsoids) of $L_{Me}Rh(COE)(MeCN)$; selected bond lengths (Å) and angles (°): Rh1–C31 2.175(2), Rh1–C38 2.115(2), Rh1–N1 2.0598(16), Rh1–N2 2.0821(18), Rh1–N40 1.9899(19), C31–C38 1.399(3), N40–C40 1.136(3); N1–Rh1–N2 89.93(7), N2–Rh1–N40 88.72(7)

between Rh and Ir. The calculated coordination strengths of σ-donors (Me_2O, MeCN) are not much smaller than those of π-acceptors, which suggests that the lack of strong THF coordination is mainly due to steric factors.

Hydrogen Complexes

Reaction of $L_{Me}Rh(COE)$ with hydrogen at –40 °C in [D_8]THF produces $L_{Me}Rh(COE)(H_2)$ (characterized by ^{1}H- and ^{13}C-NMR), the large linewidth of the hydride signal of which is suggestive of a dihydrogen complex (T_1 = 10 ms at –30 °C).[22] If the solution is allowed to warm from –40 °C to 0 °C under a hydrogen atmosphere, kept at 0 °C for a few seconds, and then cooled to –40 °C once more, the dihydrogen complex is no longer present and the dominant species (ca. 50% of the total) is a dinuclear hydride (δ_H = –24.4, J_{RhH} = 25.3 Hz), to which we tentatively assign the composition $(L_{Me}Rh)_2H_4$. This compound decomposes on attempted removal of the solvent at low temperature, and on standing in solution at room temperature, hence it could not be isolated. Deactivation of low-coordinate cationic Ir hydrogenation catalysts has also been shown to involve the formation of hydride cluster complexes.[23]

The iridium complex $L_{Me}Ir(H)$(cyclooctenyl) reacts instantaneously with hydrogen at room temperature to form the stable complex $L_{Me}Ir(COE)H_2$ (δ_H = –22.7), which does not react further with olefins and/or H_2. The X-ray structure of this complex shows a regular T-shaped coordination geometry about Ir (Figure 8). The hydrogens bound to Ir could not be located, but the narrow hydride resonance suggests that in this case we are dealing with a classical dihydride. Surprisingly, $L_{Me}Ir(COE)H_2$ is also one of the decomposition products of $L_{Me}Ir(H)$(cyclooctenyl) in solution at room temperature in the *absence* of H_2. If this decomposition is carried out in a deuterated solvent ([D_8]THF, C_6D_6), a moderate amount of the mono-deuterated complex $L_{Me}Ir(COE)HD$ is formed.[24] The H–D coupling constant of 5.6 Hz is too small for a hydrogen complex, but rather large for a dihydride.[25] The NMR spectra show effective C_{2v} symmetry at room temperature, hence the molecule must be fluxional.

The surprisingly different behaviour of the Rh and Ir complexes towards H_2 is corroborated by the calculated structures of $LRh(C_2H_4)(H_2)$ and $LIr(C_2H_4)H_2$. In both cases, only a single minimum could be located. The Rh

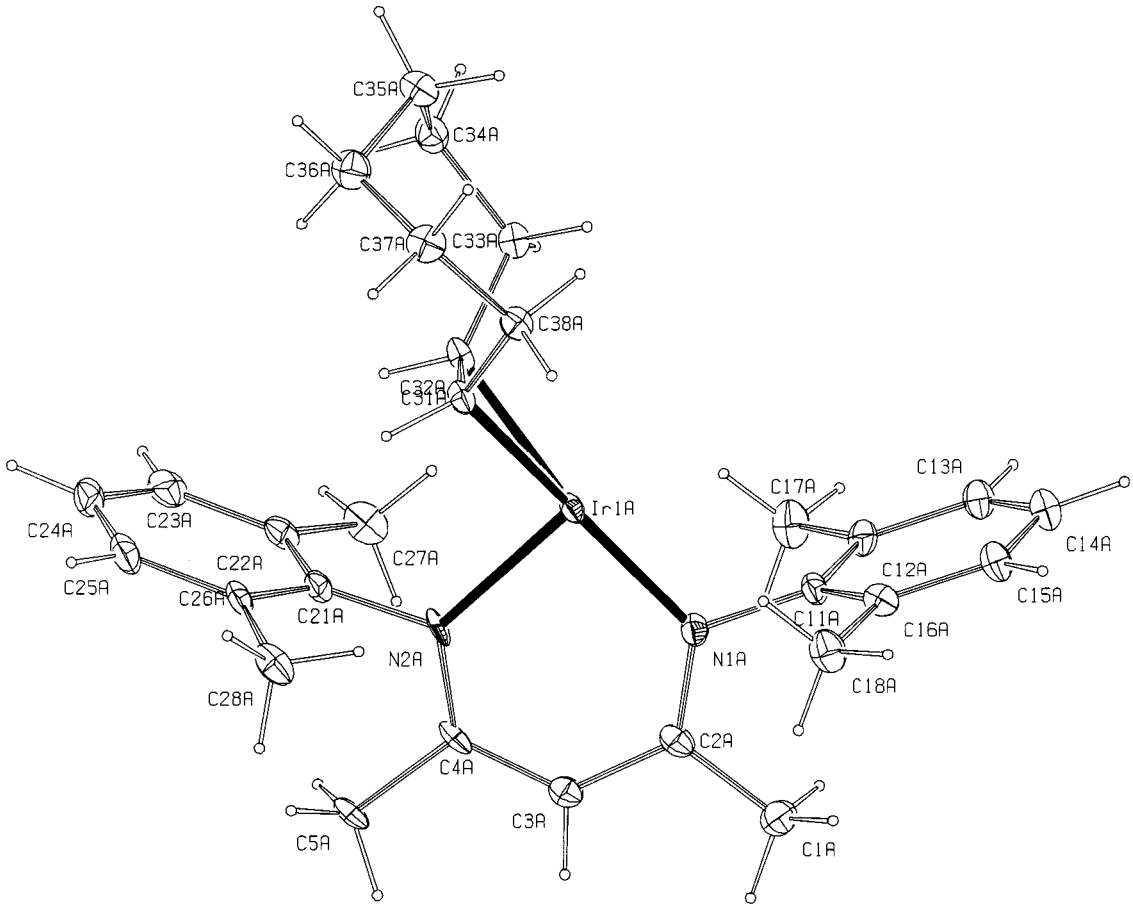

Figure 8. X-ray structure (30% ellipsoids) of $L_{Me}Ir(COE)(H_2)$; only one of the two independent molecules is shown; the hydrides were not located; selected bond lengths (Å) and angles (°): Ir1A–C31A 2.147(4), Ir1A–C32A 2.158(5), Ir1A–N1A 2.036(4), Ir1A–N2A 2.113(4), C31A–C32A 1.411(6), Ir1B–C31B 2.154(6), Ir1B–C32B 2.158(6), Ir1B–N1B 2.036(4), Ir1B–N2B 2.102(4), C31B–C32B 1.421(7); N1A–Ir1A–N2A 89.79(17), N1B–Ir1B–N2B 89.95(17)

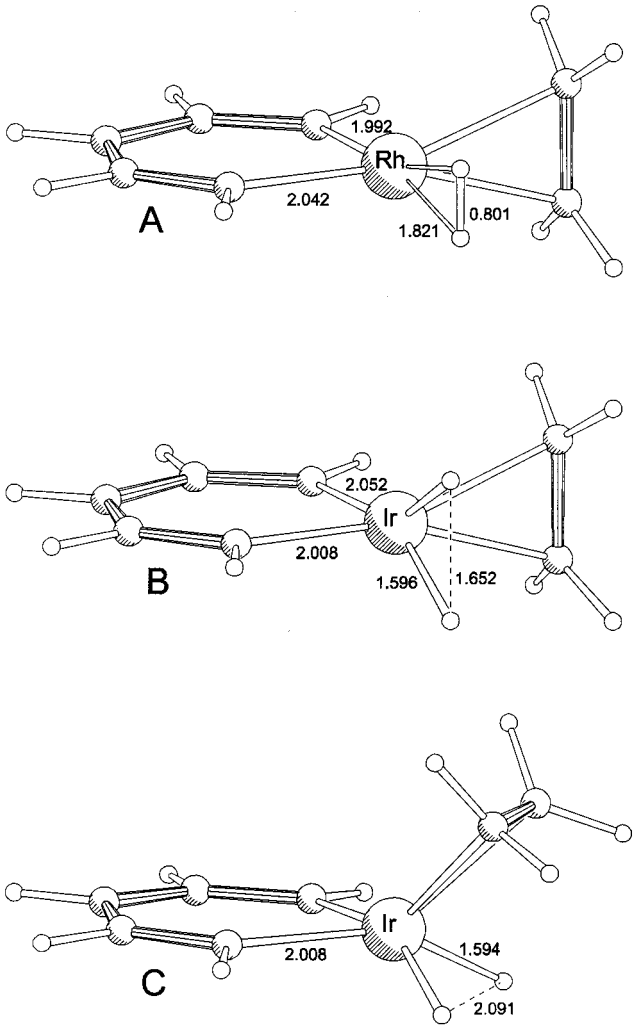

Figure 9. Calculated structures of (A) $LRh(C_2H_4)(H_2)$, (B) $LIr(C_2H_4)H_2$, and (C) the transition state for its left–right isomerization

complex (Figure 9, A) is a loosely bound (11 kcal/mol) square-planar Rh^I dihydrogen complex, in which the H–H bond is only slightly elongated (0.80 Å vs. 0.75 Å in H_2). In contrast, the Ir complex (Figure 9, B) is a strongly bound (33 kcal/mol) trigonal-bipyramidal Ir^{III} dihydride with a nonbonding (but nevertheless rather short) H–H distance of 1.65 Å. The observed fluxionality of $L_{Me}Ir(COE)H_2$ must involve a left–right shift of the olefin. The corresponding calculated transition state for $LIr(C_2H_4)H_2$ (Figure 9, C) has a square-pyramidal structure with an apical olefin ligand and an increased H–H distance of 2.09 Å. The calculated activation energy of 14 kcal/mol is compatible with this rearrangement being fast at room temperature.

Olefin Hydrogenation

$L_{Me}Rh(COE)$ is active as a catalyst in olefin hydrogenation; activity data for a few representative olefins are given in Table 2. Surprisingly, turnovers are comparable for both simple (1-hexene, cyclooctene) and highly substituted (1-methylcyclohexene, 2,3-dimethyl-2-butene) olefins. Bis(cyclohexylidene) is also hydrogenated, albeit with low turnover, but 1-*tert*-butylcyclohexene is not. The catalyst is very sensitive to impurities in the olefin or hydrogen; the turnover numbers in the table are limited by catalyst deactivation. For this reason, we have not tried to obtain kinetic data. The turnovers are not very sensitive to catalyst or olefin concentration, but do show a significant dependence on temperature (COE at 0 °C: 38 turnovers after 2 h, 49 after 4 h) and hydrogen pressure (COE at 20 bar H_2: 170 turnovers after 2 h).

In the case of cyclooctene hydrogenation, the main deactivation product was identified by NMR as $L_{Me}Rh(1,4\text{-COD})$, presumably formed from traces of 1,4-COD in the COE substrate.[26]

With 2,3-dimethyl-2-butene, the main catalyst deactivation product (ca. 90%) was a deep-green compound, which was identified as $L_{Me}Rh(OH)[\eta^3\text{-}CH_2C(Me)CMe_2]$ by NMR. Its formation can probably be attributed to trapping of an allyl hydride intermediate by traces of oxygen in the hydrogen used. Reduction of 2,3-dimethyl-2-butene with D_2 led to exclusive 1,2-deuteration; no higher deuterated species were detected. This demonstrates that olefin isomerization precedes hydrogenation. Since both cyclooctene and dimethylbutene undergo rapid isomerization according to the olefin–allyl hydride mechanism, it is reasonable to assume that this mechanism is also responsible for the isomerization during catalytic hydrogenation (Scheme 2). Hydrogenation of the trisubstituted olefin 1-methylcyclohexene might also involve an initial isomerization step.

Use of $L_{Me}Rh(COE)$ in hydrogenation is awkward because of its extreme sensitivity. However, less sensitive precursors such as $L_{Me}Rh(C_2H_4)_2$ and $L_{Me}Rh(COE)(MeCN)$ were found to give similar turnovers (see Table 2). Presumably, the active species is the same in all cases. $L_{Me}Rh(COD)$ could not be used as a precursor as it is too stable and does not react with hydrogen even at 100 °C. Catalysts derived from the L_{Cl} ligand give comparable turn-

Table 2. Olefin hydrogenation by β-diiminate Rh complexes

	Total turnover[a]		
Catalyst	cyclooctene	1-methyl-cyclohexene	2,3-dimethyl-2-butene[b]
$L_{Me}Rh(C_2H_4)_2$	77	70	43
$L_{Me}Rh(COE)$	89	44	42
$L_{Me}Rh(COE)(MeCN)$	89	n.d.	42
$L_{Cl}Rh(C_2H_4)_2$	73	42	11

[a] Neat olefin, olefin/catalyst = 125:1, 1 bar H_2, 2 h, room temperature; the catalyst was deactivated at the end of the experiment. – [b] After workup, a small amount of 2,3-epoxy-2,3-dimethylbutane was detected by GC/MS.

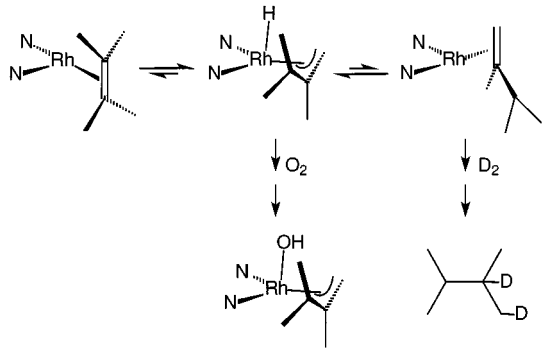

Scheme 2. Hydrogenation of 2,3-dimethyl-2-butene

overs with cyclooctene, but with the more hindered substrates the turnovers are significantly lower. We attribute this to catalyst decomposition through C–Cl oxidative addition,[27] which is able to compete with the coordination of an incoming olefin in the course of hydrogenation.

L_{Me}Ir(H)(cyclooctenyl) does not catalyze olefin hydrogenation, but merely reacts with hydrogen to form the stable dihydride L_{Me}Ir(COE)H_2, as mentioned earlier.

It is tempting to put together a catalytic cycle based on the Rh species (and their Ir analogues) observed in this work. Such a cycle is illustrated in Scheme 3. In the absence of any kinetic data, such a cycle must of course remain speculative.[28] However, it is hard to think of any realistic possibilities for ligand dissociation that would produce alternative active species. Moreover, the marginal stability of the dihydrogen complex L_{Me}Rh(COE)(H_2) is certainly compatible with its involvement in the relatively slow hydrogenation at room temperature. Here, the rate-determining step would probably be the conversion of the dihydrogen complex to a dihydride or its subsequent olefin insertion.

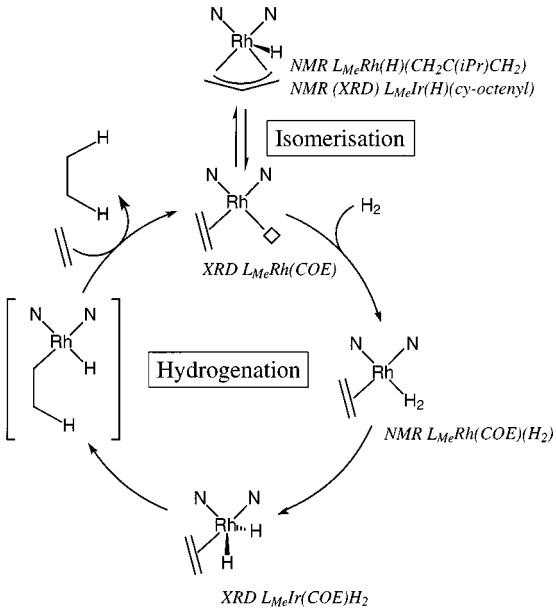

Scheme 3. Proposed cycles for olefin hydrogenation and isomerization based on the species observed; some of the steps of the hydrogenation cycle may be reversible

The cycle in Scheme 3 conforms to the "olefin route", in which the olefin is bound *before* the hydrogen.[29] This certainly happens on initiation, and, in view of the large excess of olefin and the higher calculated olefin binding energy, it most likely happens during propagation as well. However, we cannot exclude that – particularly at high conversions – a hydrogen route might become important. The precise nature of the alkane elimination step (associative or dissociative) also remains unclear.[30]

Most hydrogenation cycles involving Rh or Ir alternate between 16-*e* and 18-*e* species.[28,31] Even in cases where several active species are involved, they all go through intermediates with the same electron count. In our case, the catalysis appears to involve a 14-*e*/16-*e* mechanism, at least for the more hindered olefins, which may be attributed to steric factors.

Conclusions

Bulky β-diiminate ligands (such as L_{Me} and L_{Cl}) are good at stabilizing low coordination numbers, as demonstrated by the present work and by recent reports in the area of early transition metal chemistry. The ligand L_{Me} is particularly useful because its complexes nearly always crystallize well.[32] The ligand L_{Cl} tends to form even better crystallizing complexes, but the reactivity of the C–Cl bonds sometimes introduces complications.

The stabilization of low CN complexes by steric hindrance has allowed us to isolate a number of complexes that would normally be considered as reactive intermediates. Moreover, the use of Ir as a "model" for Rh[33] allows the direct observation of M^{III} species that for Rh would be transient intermediates in conversions between stable M^{I} species. This has allowed us to construct plausible catalytic cycles for hydrogenation and isomerization. Remarkably, the present hydrogenation appears to follow a 14-*e*/16-*e* path instead of the more usual 16-*e*/18-*e* path.

We attribute the observed stabilization of low CN complexes to the shielding of the metal atom by the vertical "walls" of the diiminate aryl groups. A perpendicular orientation of these groups is favoured by the 2,6-disubstitution pattern, which results in a strong repulsive interaction with the backbone methyl groups in a planar conformation. Indeed, work on early transition metal compounds has demonstrated dramatically increased reactivity of a low CN complex on removal of one or both of the substituents on the aryl groups.[1] However, the structure of L_{Cl}Rh(COE) shows that even 2,6-disubstituted aryl groups still have considerable freedom of movement.

One final point of interest is the observation of a pronounced agostic interaction in the L_{Me}Rh(NBE) species but not in L_{Me}Rh(COE). On the basis of both experimental and theoretical evidence, we conclude that in the former system close Rh–H contacts can easily form but do not correspond to strong bonds. Thus, caution should be exercised in equat-

ing small distances with large interaction energies. Such a conclusion is only justified in cases where the ligand undergoes considerable distortion to create the short contact.

Experimental Section

Calculations: All calculations were carried out using the Gaussian program[34] on SGI workstations. The small split-valence 3–21G basis was used for the first-row atoms.[35] For Rh and Ir, relativistic effective core potentials were used for the inner core orbitals and the LanL2DZ basis was used for the valence and outer core electrons;[36] the most diffuse *d* function in this basis was replaced by two components with exponents 1.4142 times higher and lower than the original exponent. Geometries were optimized at the RB3LYP[37] level without any constraints, unless stated otherwise.

Syntheses: All reactions were carried out under Ar. Solvents were distilled from Na/benzophenone prior to use. $[Rh(COD)Cl]_2$,[38] $[Rh(C_2H_4)_2Cl]_2$,[39] $[Rh(COE)_2Cl]_2$, and $[Ir(COE)_2Cl]_2$[40] were prepared according to literature methods.

$L_{Me}H$: A mixture of 2,6-dimethylaniline (30.5 mL, 30 g, 0.25 mol), 2,4-pentanedione (12.7 mL, 12.4 g, 0.12 mol), and *p*-toluenesulfonic acid (21.3 g) in toluene (350 mL) was refluxed for 24 h in a Dean-Stark apparatus. The toluene was then decanted off, and the solid residue was treated with diethyl ether (250 mL), water (200 mL), and $Na_2CO_3 10\ H_2O$ (53 g). After stirring for 25 min, the ether layer was separated, dried with $MgSO_4$, and the solvent was removed in vacuo. The residue was dried in vacuo (10^{-2} bar) at 100 °C for 6 h to remove any remaining free 2,6-dimethylaniline, to give 28.5 g (75%) of $L_{Me}H$. – $C_{21}H_{26}N_2$ (306.45): calcd. C 82.31, H 8.55, N 9.14; found C 81.82, H 8.71, N 8.97. – ^{1}H NMR ($CDCl_3$, 200 MHz): δ = 1.72 (1-H), 4.91 (3-H), 6.96–7.09 (m, *m*- + *p*-H), 2.19 (*o*-CH_3), 12.2 (br., NH). – $^{13}C\{^1H\}$ NMR (75.5 MHz): δ = 20.8 (C-1), 161.2 (C-2), 94.1 (C-3), 144.2 (*i*-C), 132.5 (*o*-C), 128.3 (*m*-C), 124.9 (*p*-C), 18.9 (*o*-CH_3).

$L_{Me}Li(THF)$: To a solution of LH (10 g) in THF (100 mL) was added a solution of $LiN(iPr)_2$ in THF [prepared from 1.6 M *n*-BuLi/hexane (20.5 mL) and diisopropylamine (4.6 mL)]. The solvent was subsequently removed in vacuo and the residue was crystallized from a hot toluene/hexane mixture to give 8.2 g (65%) of LLi(THF). – $C_{25}H_{33}N_2OLi$ (384.49): calcd. C 78.10, H 8.65, N 7.29; found C 78.36, H 8.52, N 7.45. – ^{1}H NMR (C_6D_6, 200 MHz): δ = 1.84 (1-H), 5.00 (3-H), 7.12 (d, *m*-H), 6.96 (t, *p*-H), 2.25 (*o*-CH_3); 2.86, 0.89 (THF). – $^{13}C\{^1H\}$ NMR (50.3 MHz): δ = 22.7 (C-1), 163.2 (C-2), 92.9 (C-3), 152.7 (*i*-C), 130.5 (*o*-C), 128.0 (*m*-C), 121.9 (*p*-C), 18.8 (*o*-CH_3); 67.7, 24.9 (THF).

$L_{Cl}H$: A mixture of 2,6-dichloroaniline (40.5 g, 0.25 mol), 2,4-pentanedione (12.7 mL, 12.4 g, 0.12 mol), and *p*-toluenesulfonic acid (21.3 g) in toluene (350 mL) was refluxed for 24 h in a Dean-Stark apparatus. The toluene was then decanted off, and the solid residue was treated with diethyl ether (250 mL), water (200 mL), and $Na_2CO_3 10\ H_2O$ (53 g). After stirring for 25 min, the ether layer was separated, dried with $MgSO_4$, and the solvent was removed in vacuo. The residue was dried in vacuo (10^{-2} bar) at 100 °C for 6 h to remove any remaining free 2,6-dichloroaniline, and the residue was crystallized from heptane to give 34 g (70%) of $L_{Cl}H$. – $C_{17}H_{14}N_2Cl_4$ (388.12): calcd. C 52.61, H 3.64, N 7.22, Cl 36.54; found C 52.74, H 3.67, N 7.38, Cl 36.43. – ^{1}H NMR ($CDCl_3$, 200 MHz): δ = 1.71 (1-H), 4.94 (3-H), 7.17 (d, *m*-H), 6.86 (t, *p*-H), 12.0 (NH). – $^{13}C\{^1H\}$ NMR (50.3 MHz): δ = 21.4 (C-1), 163.1 (C-2), 95.9 (C-3), 141.1 (*i*-C), 131.7 (*o*-C), 128.6 (*m*-C), 126.2 (*p*-C).

$L_{Cl}Li(THF)$: To a solution of $L_{Cl}H$ (12.6 g) in THF (100 mL) was added a solution of $LiN(iPr)_2$ in THF [prepared from 1.6 M *n*-BuLi/hexane (20.5 mL) and diisopropylamine (4.6 mL)]. The solvent was subsequently removed in vacuo, and the residue was crystallized from a hot toluene/hexane mixture to give 12.2 g (80%) of yellow $L_{Cl}Li(THF)$. – $C_{21}H_{21}N_2OCl_4Li$ (466.16): calcd. C 54.11, H 4.54, N 6.01, Cl 30.42; found C 54.06, H 4.59, N 6.13, Cl 30.54. – ^{1}H NMR (C_6D_6, 200 MHz): δ = 1.82 (1-H), 4.93 (3-H), 7.02 (d, *m*-H), 6.32 (t, *p*-H); 2.96, 0.82 (THF). – $^{13}C\{^1H\}$ NMR (50.3 MHz): δ = 23.5 (C-1), 165.6 (C-2), 95.6 (C-3), 149.5 (*i*-C), 130.7 (*o*-C), 128.7 (*m*-C), 123.0 (*p*-C); 68.2, 25.2 (THF).

$L_{Me}Rh(1,5\text{-}COD)$: A solution of $L_{Me}Li(THF)$ (1.0 g) in THF (10 mL) was added to a suspension of $[Rh(1,5\text{-}COD)Cl]_2$ (0.64 g) in THF (5 mL). The resulting mixture was stirred at room temperature for 2 h, and then the solvent was removed in vacuo. The residue was crystallized from benzene/hexane (2:1) (the hot solution was filtered to remove LiCl) to give yellow crystals of $L_{Me}Rh(1,5\text{-}COD)$ (1.2 g, 88%). – $C_{29}H_{37}N_2Rh$ (516.53): calcd. C 67.43, H 7.22, N 5.42; found C 67.42, H 7.38, N 5.42. – ^{1}H NMR ($CDCl_3$, 200 MHz): δ = 1.55 (1-H), 5.10 (3-H), 6.97–7.11 (m, *m*- + *p*-H), 2.31 (*o*-CH_3), 3.01 (br., CH=CH), 2.12, 1.60 (CH_2). – $^{13}C\{^1H\}$ NMR (50.3 MHz): δ = 25.5 (C-1), 159.3 (C-2), 97.8 (C-3), 150.9 (*i*-C), 132.9 (*o*-C), 128.7 (*m*-C), 124.9 (*p*-C), 19.3 (*o*-CH_3), 79.8 (CH=CH, J_{RhC} = 13 Hz), 31.1 (CH_2).

$L_{Cl}Rh(1,5\text{-}COD)$: A solution of $L_{Cl}Li(THF)$ (0.5 g) in THF (10 mL) was added to a suspension of $[Rh(1,5\text{-}COD)Cl]_2$ (0.26 g) in THF (5 mL). The resulting mixture was stirred at room temperature for 4 h, and then the solvent was removed in vacuo. The residue was crystallized from toluene (70/–20 °C; the hot solution was filtered to remove LiCl) to give yellow crystals of $L_{Cl}Rh(1,5\text{-}COD)$ (0.32 g, 50%). – $C_{25}H_{25}N_2Cl_4Rh$ (598.20): calcd. C 50.20, H 4.21, N 4.68, Cl 23.71; found C 50.14, H 4.12, N 4.69, Cl 23.57. – ^{1}H NMR (C_6D_6, 200 MHz): δ = 1.72 (1-H), 5.28 (3-H), 7.14 (d, *m*-H), 6.45 (t, *p*-H), 3.61 (br., CH=CH), 2.33, 1.56 (m, CH_2). – $^{13}C\{^1H\}$ NMR (50.3 MHz): δ = 25.1 (C-1), 160.9 (C-2), 99.3 (C-3), 147.8 (*i*-C), 132.9 (*o*-C), 128.5 (*m*-C), 125.8 (*p*-C), 78.8 (CH=CH, J_{RhC} = 13 Hz), 30.8 (CH_2).

$L_{Me}Rh(C_2H_4)_2$: A solution of $L_{Me}Li(THF)$ (1.0 g) in THF (10 mL) was added to a suspension of $[Rh(C_2H_4)_2Cl]_2$ (0.51 g) in THF (5 mL). The resulting mixture was stirred at room temperature for 2 h, and then the solvent was removed in vacuo. The residue was crystallized from diethyl ether (30/–20 °C; the warm solution was filtered to remove LiCl) to give very large, dark brown-yellow crystals of $L_{Me}Rh(C_2H_4)_2$ (0.68 g, 50%). Small crystals or powdered material are yellow. – $C_{25}H_{33}N_2Rh$ (464.45): calcd. C 64.54, H 7.16, N 6.03; found C 64.77, H 7.22, N 6.16. – ^{1}H NMR (C_6D_6, 200 MHz): δ = 1.65 (1-H), 5.30 (3-H), 7.04–7.12 (m, *m*- + *p*-H), 2.41 (*o*-CH_3), 2.62, 2.01 (m, C_2H_4). – $^{13}C\{^1H\}$ NMR (50.3 MHz): δ = 25.9 (C-1), 159.5 (C-2), 98.9 (C-3), 150.4 (*i*-C), 133.0 (*o*-C), 129.2 (*m*-C), 125.7 (*p*-C), 19.8 (*o*-CH_3), 63.3 (C_2H_4, J_{RhC} = 11 Hz).

$L_{Cl}Rh(C_2H_4)_2$: A solution of $L_{Cl}Li(THF)$ (0.5 g) in THF (10 mL) was added to a suspension of $[Rh(C_2H_4)_2Cl]_2$ (0.21 g) in THF (5 mL). The resulting mixture was stirred at room temperature for 2 h, and then the solvent was removed in vacuo. The residue was crystallized from diethyl ether (30/–20 °C; the warm solution was filtered to remove LiCl) to give dark-red crystals of $L_{Cl}Rh(C_2H_4)_2$ (0.22 g, 36%). – $C_{21}H_{21}N_2Cl_4Rh$ (546.13): calcd. C 46.19, H 3.88, N 5.13, Cl 25.97; found C 46.21, H 3.89, N 5.25, Cl 25.85. – ^{1}H NMR (C_6D_6, 200 MHz): δ = 1.73 (1-H), 5.29 (3-H), 7.05 (d, *m*-

H), 6.44 (t, *p*-H), 2.88, 2.02 (m, C_2H_4). – $^{13}C\{^1H\}$ NMR (125.76 MHz): δ = 24.2 (C-1), 159.9 (C-2), 98.1 (C-3), 146.1 (*i*-C), 131.8 (*o*-C), 127.4 (*m*-C), 125.0 (*p*-C), 60.8 (C_2H_4, J_{RhC} = 12 Hz).

L_{Me}Rh(COE): A solution of L_{Me}Li(THF) (3.24 g) in THF (10 mL) was added to a suspension of $[Rh(COE)_2Cl]_2$ (3.03 g) in THF (5 mL). The resulting mixture was stirred at room temperature for 1 day, and then the solvent was removed in vacuo. The residue was extracted with two 50 mL portions of warm hexane (60 °C), the combined extracts were concentrated to a volume of 15 mL, and cooled to –20 °C. The next day, a crop of dark-violet crystals had formed. These crystals were recrystallized from fresh hexane to give 3.0 g (66%) of L_{Me}Rh(COE). Crystals suitable for X-ray diffraction analysis were obtained by slow crystallization from cyclohexane. – $C_{29}H_{39}N_2Rh$ (518.55): calcd. C 67.17, H 7.58, N 5.40; found C 67.04, H 7.41, N 5.57. – ^1H NMR (200 MHz, C_6D_{12}, room temp.): δ = 1.72 (1-H), 5.18 (3-H), 7.0–7.1 (m, *m*- + *p*-H), 2.65 (*o*-CH_3), 1.87 (br. s, 8 H), 0.34 (br. s, 6 H) cyclooctene. – ^1H NMR (500 MHz, $[D_8]$THF, –80 °C): δ = 1.55, 1.39 (1-,1′-H), 4.95 (3-H), 7.16, 7.10 (*m*-,*m*′-H), 7.06, 7.05 (*p*-,*p*′-H), 2.70, 2.39 (*o*,*o*′-CH_3), 2.48 (CH=CH), 2.08, 1.5, 1.2, 1.0 (br., CH_2). – $^{13}C\{^1H\}$ NMR (125.7 MHz, $[D_8]$THF, –80 °C): δ = 24.1 (C-1), 26.5 (C-1′, superimposed by solvent signal), 158.6, 156.3, 154.3, 150.9 (C-2, C-2′, *i*-,*i*′-C), 100.4 (C-3, J_{RhC} = 39 Hz), 134.6, 134.5 (*o*-,*o*′-C), 129.9, 129.5 (*m*-,*m*′-C), 126.2, 125.8 (*p*-,*p*′-C), 21.1, 20.4 (*o*,*o*′-CH_3), 64.8 (br., CH=CH), 31.6 (br., CH_2); remaining CH_2 groups not observed.

L_{Me}Ir(cyclooctenyl)(H): A solution of L_{Me}Li(THF) (1.0 g) in diethyl ether (10 mL) was added to a suspension of $[Ir(COE)_2Cl]_2$ (1.16 g) in diethyl ether (5 mL). The resulting mixture was stirred at room temperature for 4 h, and then the solvent was removed in vacuo. The residue was extracted with two 20 mL portions of hexane, the combined extracts were concentrated to a volume of 8 mL, and cooled to –20 °C. After 3 days, orange-red crystals had formed. Concentration of the mother liquor to 3 mL and cooling to –20 °C produced a second crop of crystals. The crystals were dried in vacuo and stored at –20 °C. – $C_{29}H_{39}N_2Ir$ (607.86): calcd. C 57.30, H 6.47, N 4.61; found C 57.08, H 6.56, N 4.74. – ^1H NMR ($[D_8]$THF, –20 °C, 400 MHz): δ = 1.70 (1-H), 5.37 (3-H), 7.20, 7.18 (d, *m*- + *m*′-H), 6.99 (t, *p*-H), 2.16, 2.21 (*o*,*o*′-CH_3), 5.40 (t, 1 H), 2.54 (br. q, 2 H, cyclooctenyl CH), 1.90, 1.27, 1.05, 0.82, 0.25 (br. m, CH_2), –46.19 (IrH). – $^{13}C\{^1H\}$ (100.6 MHz): δ = 23.9 (C-1), 157.6 (C-2), 103.2 (C-3), 157.2 (*i*-C), 132.7, 130.9 (*o*-,*o*′-C), 130.2, 129.8 (*m*-,*m*′-C), 126.0 (*p*-C), 20.3, 20.0 (*o*,*o*′-CH_3), 84.9, 49.6 (cyclooctenyl CH), 32.8, 30.3, 19.9 (CH_2). – IR (KBr): $\tilde{\nu}_{Ir-H}$ = 2122 cm^{-1}.

L_{Cl}Rh(COE): A solution of L_{Cl}Li(THF) (2.0 g) in THF (10 mL) was added to a suspension of $[Rh(COE)_2Cl]_2$ (1.54 g) in THF (10 mL). The resulting mixture was stirred at room temperature for 1 h, and then the solvent was removed in vacuo. The residue was extracted with two 50 mL portions of hexane, the combined extracts were concentrated to dryness in vacuo, and the residue was redissolved in diethyl ether (50 mL). This solution was filtered and then concentrated to a volume of 4 mL and stored overnight at –20 °C. Thereafter, fine red needles had formed, which were filtered off and dried in vacuo to give 0.77 g (30%) of L_{Cl}Rh(COE). – $C_{25}H_{27}N_2Cl_4Rh$ (600.22): calcd. C 50.03, H 4.53, N 4.67, Cl 23.63; found C 49.86, H 4.54, N 4.80, Cl 23.63. – ^1H NMR (200 MHz, C_6D_6, 25 °C): δ = 6.96 (d, 4 H, *m*-H), 6.34 (t, 2 H, *p*-H), 5.36 (s, 1 H, 3-H), 2.2 (v. br., 8 H, COE *exo* ± vinylic), 1.89 (s, 1-H), 1.47 (br., 6 H, COE *endo*). – ^1H NMR (500.13 MHz, $[D_8]$THF, –53 °C[8]): δ = 7.48, 7.39 (m, 2 H each, *m*-,*m*′-H), 7.22, 6.90 (m, 1 H each, *p*-,*p*′-H), 5.30 (s, 1 H, 3-H), 2.20, 1.58 (s, 3 H each, 1-,1′-H), 1.1–2.6 (overlapping multiplets, 14 H, COE). – $^{13}C\{^1H\}$ NMR (125.76 MHz, $[D_8]$THF, –53 °C[8]): δ = 162.5, 162.2 (2-C, 2′-C), 151.7, 146.5 (*i*-,*i*′-C), 133.5, 130.4 (*o*-,*o*′-C), 129.9 (*m*-,*m*′-C), 128.8, 123.7 (*p*-,*p*′-C), 106.6 (C-3), 32.6, 28.2 (COE), 24.6 (C-1); C-1′ and remaining COE resonances not observed.

L_{Me}Rh(C_2Me_4): A suspension of L_{Me}Rh(COE) (0.15 g) in C_2Me_4 (7 mL) was stirred under a hydrogen atmosphere (1 bar) until the solid had completely dissolved (ca. 3 min), giving a dark-brown solution. All volatiles were then removed in vacuo, and the residue was redissolved in $[D_8]$THF for NMR studies (see Results Section). The solution gave rise to small but sharp peaks due to the oxidation product $L_{Me}Rh[\eta^3\text{-}CH_2C(Me)CMe_2](OH)$ (see below); resonances due to the main product were found to be broad at room temperature. At 243 K, all peaks due to the main component $L_{Me}Rh[\eta^3\text{-}CH_2C(iPr)CH_2](H)$ could be assigned: ^1H NMR ($[D_8]$THF, 500 MHz, 243 K): δ = 1.56 (obscured by cyclooctane signal; 1-H), 5.04 (3-H), 7.02, 7.04 (d, *m*-H), 6.90 (t, *p*-H), 2.53, 2.23 (*o*-CH_3), 1.85 (br. sept, H*i*Pr), 1.24 (br. d, CMe_2), –2.45 (br., CH_2 + Rh–H). – $^{13}C\{^1H\}$ NMR (125.7 MHz): δ = 23.4 (C-1), 157.6 (C-2), 99.6 (C-3), 156.8 (*i*-C), 135.0, 131.3 (*o*-C), 129.5 (*m*-C), 126.1 (*p*-C), 19.9, 21.2 (*o*-CH_3), 97.1 (C*i*Pr, J_{RhC} = 11 Hz) (CH_2 obscured by THF), 36.0 (CMe_2), 23.8 (CMe_2). In addition, some peaks due to the minor component $L_{Me}Rh[\eta^3\text{-}CH_2C(Me)CMe_2](H)$ could be tentatively assigned: ^1H NMR (500 MHz, 218 K): δ = 5.03 (3-H), –12.17 (RhH). – $^{13}C\{^1H\}$ NMR (125.7 MHz, 243 K): δ = 158.4 (C-2), 156.4, 155.9 (*i*-,*i*′-C), 133.1 (*o*-C), 130.0, 129.7, 129.3 (*m*-C), 126.4 (*p*-C), 100.0 (C-3), 21.9, 21.1, 20.5 (*o*-CH_3).

L_{Me}Rh(NBE): To a solution of L_{Me}Rh(COE) (0.7 g) in hexane (5 mL) was added NBE (0.5 g). The resulting mixture was stirred at room temperature for 15 min. All volatiles were then removed in vacuo, and the residue was crystallized from hexane (50/–20 °C) to give 0.56 g (83%) of brown-red L_{Me}Rh(NBE). – $C_{28}H_{35}N_2Rh$ (502.50): calcd. C 66.93, H 7.02, N 5.57; found C 66.68, H 6.82, N 5.42. – ^1H NMR (200 MHz, C_6D_{12}): δ = 1.40, 1.60 (1-H), 4.96 (3-H), 6.8–6.9 (m, *m*- + *p*-H), 2.31, 2.61 (*o*-CH_3), 2.55, 2.71 (vinylic and bridgehead H), 0.75 (CH_2CH_2), –0.82 (d, $^2J_{HH}$ = 14.5 Hz, nonagostic HCH), –10.2 (dd, $^2J_{HH}$ = 14.5, J_{RhH} = 11.7 Hz, agostic HCH). – $^{13}C\{^1H\}$ NMR (50.4 MHz, C_6D_{12}): δ = 23.5, 20.9 (C-1), 156.9, 155.7 (C-2), 99.2 (C-3), 158.6, 156.3, 153.3, 150.3 (*i*-C), 133.2 (*o*-C), 128.7, 128.6 (*m*-C), 125.5, 125.2 (*p*-C), 19.9, 19.4 (*o*-CH_3), 65.7 (d, C=C, J_{RhC} = 15 Hz), 47.5 (bridgehead), 29.6 (CH_2CH_2), 16.0 (CH_2). – ^{13}C NMR (125.7 MHz, C_6D_{12}): $^1J_{CH}$ = 108 and 141 Hz for the NBE CH_2. The infrared spectrum (KBr and Nujol mull) did not show any distinct peaks attributable to the agostic C–H bond.

L_{Me}Rh(COE)(N_2): Solutions of L_{Me}Rh(COE)(N_2) were generated by preparing NMR samples of L_{Me}Rh(COE) under nitrogen atmosphere. – ^1H NMR ($[D_8]$THF, 500 MHz): δ = 1.56, 1.75 (1-,1-H′), 5.24 (3-H), 7.16, 7.15 (d, *m*-,*m*′-H), 7.04, 7.09 (t, *p*-,*p*′-H), 2.50, 2.32 (*o*,*o*′-CH_3), 3.04 (CH=CH), 2.14, 1.59, 1.2 (br., CH_2). – $^{13}C\{^1H\}$ NMR (125.7 MHz): δ = 26.6, 23.8 (C-1, C-1′), 160.3, 159.1 (C-2, C-2′), 99.9 (C-3, J_{RhC} = 11 Hz), 156.2, 150.0 (*i*-,*i*′-C), 134.8, 133.3 (*o*-,*o*′-C), 130.1, 29.8 (*m*-,*m*′-C), 127.1, 126.6 (*p*-,*p*′-C), 20.6, 20.1 (*o*,*o*′-CH_3), 76.7 (CH=CH, J_{RhC} = 11 Hz), 32.5, 30.8, 28.1 (CH_2). Essentially pure solid L_{Me}Rh(COE)(N_2) was prepared by dissolving L_{Me}Rh(COE) (0.1 g) in hexane (1 mL) under nitrogen, concentrating the solution to a volume of 0.3 mL in vacuo, and connecting the Schlenk tube to another one containing 6 mL of paraffin oil. After 6 weeks, the hexane had diffused into the paraffin oil and the oily residue had solidified. – IR (Nujol mull): $\tilde{\nu}_{N-N}$ = 2172 cm^{-1}.

$L_{Me}Rh(COE)(MeCN)$: A solution of $L_{Me}Li(THF)$ (0.51 g) in THF (6 mL) was added to a suspension of $[Rh(COE)_2Cl]_2$ (0.48 g) in THF (3 mL) and MeCN (0.75 mL). The resulting mixture was stirred for one day and then the solvents were removed in vacuo. The residue was extracted with two 20 mL portions of cyclohexane. The combined extracts were concentrated to a volume of 10 mL and stored for overnight at 6 °C, which led to the deposition of a yellow powder (0.56 g, 75%). Crystals suitable for X-ray diffraction were obtained by slow crystallization at room temperature. – $C_{31}H_{42}N_3Rh$ (559.60): calcd. C 66.54, H 7.56, N 7.51; found C 66.32, H 7.91, N 7.48. – ^{1}H NMR (C_6D_6, 293 K, 200 MHz): δ = 6.93 (m, *m*-,*p*-H), 5.19 (3-H), 2.80, 2.25, 1.52, 1.27 (m, COE), 2.54, 2.42 (*o*,*o*′-CH_3), 1.69, 1.52 (1-,1′-H), 0.45 (MeCN). – $^{13}C\{^1H\}$ NMR (50.4 MHz): δ = 158.0, 156.0 (C-2, C-2′), 154.3, 149.4 (*i*-,*i*′-C), 133.1, 132.8 (*o*-,*o*′-C), 128 (superimposed by solvent signal, *m*-H), 124.5, 123.2 (*p*-,*p*′-C), 116.1 (CH_3CN), 98.0 (C-3), 66.9 (d, J_{RhC} = 14 Hz, CH=CH), 31.0, 29.7, 26.9 (COE), 25.3, 23.08 (1-,1′-C), 19.5, 19.0 (*o*,*o*′-CH_3), 1.4 (CH_3CN).

$L_{Me}Rh(1,4\text{-}COD)$: $L_{Me}Rh(COE)$ (0.3 g) was dissolved in 1,3-COD (2 mL) and the solution was stirred for 10 min. The solvent was then removed in vacuo, leaving essentially pure $L_{Me}Rh(1,4\text{-}COD)$, which was characterized only by NMR. Heating of the solution in 1,3-COD to 40 °C for 10 min prior to workup resulted in formation of $L_{Me}Rh(1,5\text{-}COD)$. – ^{1}H NMR (C_6H_6, 293 K, 200 MHz): δ = 7.0–7.2 (m, *m*-,*p*-H), 5.25 (3-H), 3.26, 2.7, 2.4, 2.1, 1.7, 1.2 (br. m, 1,4-COD), 2.48, 2.41 (*o*-CH_3), 1.66 (1-H). – $^{13}C\{^1H\}$ NMR (50.3 MHz): δ = 158.3 (C-2), 150.4 (*i*-C), 133.2, 131.8 (*o*-,*o*′-C), 128 (obscured by solvent signal, *m*-,*m*′-C), 124.7 (*p*-C), 98.2 (C-3), 24.9 (C-1), 19.2, 18.9 (*o*,*o*′-CH_3), 72.4 (d, J_{RhC} = 14 Hz), 51.1 (d, J_{RhC} = 8 Hz, C=C), 29.1 (2 C), 28.3, 25.7 (CH_2). The same material remained following hydrogenation of COE with $L_{Me}Rh(COE)$.

$L_{Me}Rh[CH_2C(Me)CMe_2](OH)$: Following hydrogenation experiments with 2,3-dimethyl-2-butene, this compound remained as a deep-green oil. All attempts to crystallize it were unsuccessful. – ^{1}H NMR (C_6H_6, 293 K, 200 MHz): δ = 6.9–7.2 (m, *m*-,*p*-H), 5.26 (3-H), 3.61, 1.84 (br. s, CH_2), 2 × 2.74, 2.57, 2.34 (*o*-CH_3), 1.84, 1.58 (1-H), 1.42, 0.73, 0.50 ($CMeCMe_2$), –1.33 (OH). – $^{13}C\{^1H\}$ NMR (75.5 MHz): δ = 156.9, 153.4 (C-2, C-2′), 153.0, 149.7 (*i*-,*i*′-C), 133.5, 132.9, 132.4, 132.3 (*o*-C), 128 (obscured by solvent signal, *m*-C), 124.4, 124.1 (*p*-,*p*′-C), 98.6 (C-3), 89.9 ($CH_2CMeCMe_2$), 67.7 (d, J_{RhC} = 12 Hz, $CH_2CMeCMe_2$), 50.7 (d, J_{RhC} = 14 Hz, $CH_2CMeCMe_2$), 23.4, 21.4 (C-1, C-1′), 19.4, 19.3, 19.2, 18.8 (*o*-CH_3), 29.0, 26.4, 17.3 ($CH_2CMeCMe_2$).

$L_{Me}Rh(COE)(H_2)$: A solution of $L_{Me}Rh(COE)$ (0.12 g) in $[D_8]$THF (0.7 mL) was cooled to –40 °C and then stirred under hydrogen atmosphere (1 bar) for 3 min. The solution was then cooled to –80 °C and transferred to a cooled NMR tube under Ar. NMR studies showed it to contain $L_{Me}Rh(COE)(H_2)$ as the main Rh complex (ca. 75% of the total; the remainder was $[L_{Me}RhH_2]_2$; see below). – ^{1}H NMR ($[D_8]$THF, 243 K, 500 MHz): δ = 1.51, 1.56 (obscured by cyclooctane signal, 1-,1′-H), 5.12 (3-H), 7.11, 7.02 (d, *m*-,*m*′-H), 7.00, 6.90 (t, *p*-,*p*′-H), 2.39, 2.28 (*o*,*o*′-CH_3), 2.45 (CH=CH), 2.12, 1.59, 1.3 (br., CH_2), –12.8 (br., Rh–H_2; T_1 = 10 ms by inversion-recovery). – $^{13}C\{^1H\}$ NMR (125.7 MHz): δ = 25.8, 22.8 (C-1, C-1′), 160.7, 160.2 (C-2, C-2′), 99.9 (C-3), 158.7, 151.1 (*i*-,*i*′-C), 133.7, 132.1 (*o*-,*o*′-C), 130.1, 129.7 (*m*-,*m*′-C), 126.7, 126.1 (*p*-,*p*′-C), 20.9, 20.2 (*o*,*o*′-CH_3), 76.1 (CH=CH, J_{RhC} = 12 Hz), 35.7, 33.3, 28.0 (CH_2).

$[L_{Me}RhH_2]_2$: The aforementioned solution of (mainly) $L_{Me}Rh(COE)(H_2)$ was transferred back to a Schlenk tube and then warmed (with stirring) to 0 °C under hydrogen atmosphere. After stirring at 0 °C for 10 min, the solution was cooled to –40 °C once more, whereupon NMR spectra were recorded. All the $L_{Me}Rh(COE)(H_2)$ was seen to have been consumed; the solution contained $[L_{Me}RhH_2]_2$ as the main Rh complex (ca. 50% of the total), accompanied by a large number of other compounds in low concentrations. The compound decomposed on standing and on evaporation of the solvent, and all attempts to isolate it were unsuccessful. – ^{1}H NMR ($[D_8]$THF, 243 K, 500 MHz): δ = 1.26 (1-H), 4.94 (3-H), 6.80 (d, *m*-H), 7.02 (t, *p*-H), 1.74 (superimposed by THF signal, *o*-CH_3), –24.23 (t, Rh–H_2, J_{RhHav} = 25 Hz). – $^{13}C\{^1H\}$ NMR (125.7 MHz): δ = 23.6 (C-1), 158.7 (C-2), 100.9 (C-3), 154.3 (*i*-C), 133.8 (*o*-C), 131.2 (*m*-C), 125.3 (*p*-C), 19.8 (*o*-CH_3).

$L_{Me}Ir(COE)H_2$: $L_{Me}Ir(cyclooctenyl)(H)$ (0.2 g) was dissolved in THF (4 mL) and the solution was stirred under hydrogen (1 bar) for 10 min. The volatiles were then removed in vacuo. The reaction was clean and virtually quantitative according to ^{1}H-NMR, but the product was found to be very soluble, even in pentane. X-ray quality crystals were obtained by dissolving the residue in pentane, concentrating the solution to a volume of 0.25 mL, and slowly cooling it to –20 °C. – ^{1}H NMR (C_6D_6, 293 K, 200 MHz): δ = 1.50 (1-H), 5.26 (3-H), 6.96 (d, *m*-H), 6.81 (t, *p*-H), 2.22 (*o*-CH_3), 2.62 (CH=CH), 2.04 (br., =CH–CH_2 *exo*), 0.9–1.3 (br., all other CH_2), –22.6 (IrH_2), –22.74 (IrHD, J_{HD} = 5.6 Hz). – $^{13}C\{^1H\}$ NMR (125.7 MHz): δ = 23.7 (br., C-1), 161 (br., C-2), 102.5 (C-3) (*i*-C not observed), 131.7 (*o*-C), 127.8 (*m*-C), 125.9 (*p*-C), 19.2 (*o*-CH_3), 62.2 (CH=CH), 35.3, 33.2, 26.7 (CH_2). – IR (KBr): $\tilde{\nu}_{Ir-H}$ = 2217 cm^{-1}.

Hydrogenation Experiments

Olefins (COE, 1-methylcyclohexene, 2,3-dimethyl-2-butene, 1-*tert*-butylcyclohexene) were dried over Na and then transferred to a cold trap in vacuo prior to use. The catalyst (ca. 50 mg) was dissolved in neat olefin (1 mL), and the solution was stirred under 1 bar of hydrogen for 2 h. By that time, no more hydrogen was being absorbed. The resulting solution was filtered through alumina to remove Rh and ligand residues, and subsequently analyzed by ^{1}H- and ^{13}C-NMR. Hydrogenation of the solid olefin bis(cyclohexylidene) was carried out in pentane solution [bis(cyclohexylidene) (0.3 g) and $L_{Me}Rh(COE)$ (0.095 g) in pentane (3 mL)]: 5 turnovers (50% conversion) after 2 h (by ^{13}C-NMR).

X-ray Structure Determinations

Crystals were mounted in thin-walled glass capillaries under Ar. Details of all structure determinations are collected in Table 3. Since the glass capillaries prevented an accurate description of the crystal shapes, empirical absorption corrections[41] were applied in most cases (see Table 3). Structures were solved using the PATTY option[42] of the DIRDIF program system.[43] Refinements were carried out with the SHELXL-97 package.[44] All nonhydrogen atoms were refined with anisotropic temperature factors. The hydrogen atoms were placed in calculated positions and refined isotropically in riding mode. All refinements were made by full-matrix least-squares on F^2. Unless otherwise noted, geometrical calculations[45] revealed neither unusual geometric features, nor unusually short intermolecular contacts. Moreover, the calculations revealed no higher symmetry and no solvent accessible areas.

Remarks for Specific Structures. –$L_{Me}Rh(C_2H_4)_2$: The hydrogens of the ethene moieties were freely refined. $L_{Cl}Rh(COE)$: The crystal showed considerable decay (up to 25%) during the measurements, resulting in somewhat higher *R* indices. $L_{Me}Rh(COD)$ and $L_{Me}Rh(COE)(MeCN)$: All hydrogen atoms were freely refined in the final cycles.

Table 3. Details of X-ray structure determinations

Compound	$L_{Me}Rh(COD)$	$L_{Me}Rh(C_2H_4)_2$	$L_{Cl}Rh(COE)$	$L_{Me}Rh(NBE)$	$L_{Me}Rh(COE)(MeCN)$	$L_{Me}Ir(COE)H_2$
Crystal color	transparent brownish	transparent orange-red	transparent orange-brown-red	dark brown-black	transparent yellow-brown	transparent light brown-yellow
Crystal shape	regular fragment	irregular thick platelet	irregular platelet	irregular fragment	irregular fragment	irregular fragment
Crystal size (mm)	0.33 × 0.33 × 0.31	0.51 × 0.45 × 0.16	0.50 × 0.12 × 0.04	0.40 × 0.33 × 0.30	0.50 × 0.22 × 0.22	0.33 × 0.21 × 0.13
Empirical formula	$C_{29}H_{37}N_2Rh$	$C_{25}H_{33}N_2Rh$	$C_{25}H_{27}Cl_4N_2Rh$	$C_{28}H_{35}N_2Rh$	$C_{31}H_{42}N_3Rh$	$C_{29}H_{41}IrN_2$
Formula weight	516.52	464.44	600.20	502.49	559.59	609.84
Temperature [K]	293(2)	208(2)	293(2)	293(2)	150(2)	150(2)
Radiation (graphite mon.)	Mo-K_α	Cu-K_α	Cu-K_α	Cu-K_α	Mo-K_α	Mo-K_α
Wavelength [A]	0.71073	1.54184	1.54184	1.54184	0.71073	0.71073
Crystal system, space group	monoclinic, *C*2/*c*	monoclinic, *P*21/*n*	monoclinic, *P*21/*n*	monoclinic, *P*21/*n*	monoclinic, *P*21/*c*	monoclinic, *P*21/*a*
Unit cell # reflections, θ range [°]	25, 18.506 to 20.343	25, 40.342 to 46.309	25, 12.225 to 19.413	25, 18.704 to 45.402	20212, 1.660 to 26.330	45537, 1.730 to 27.450
a [Å]	14.0042(10)	13.3932(3)	18.705(2)	14.0623(5)	12.7445(2)	17.4950(4)
b [Å]	13.4813(9)	13.4621(3)	7.4768(11)	13.0771(13)	14.6992(4)	14.0151(2)
c [Å]	13.456(4)	13.6582(4)	37.051(6)	14.4341(8)	15.7950(4)	23.0605(6)
α [°]	90	90	90	90	90	90
β [°]	97.187(12)	114.3825(19)	101.939(13)	112.441(4)	106.0702(12)	108.6013(9)
γ [°]	90	90	90	90	90	90
Volume [Å^3]	2520.4(8)	2242.94(10)	5069.7(13)	2453.4(3)	2843.31(11)	5358.9(2)
Z, calcd. density [Mgm^{-3}]	4, 1.361	4, 1.375	8, 1.573	4, 1.360	4, 1.307	8, 1.512
Abs. Coefficient μ [mm^{-1}]	0.696	6.227	9.448	5.737	0.623	5.001
Diffractometer	Enraf–Nonius CAD4	Enraf–Nonius CAD4	Enraf–Nonius CAD4	Enraf–Nonius CAD4	Nonius KappaCCD	Nonius KappaCDD
Scan	θ/2θ	θ/2θ	θ/2θ	θ/2θ	area detector φ and ω	area detector φ and ω
F(000)	1080	968	2432	1048	1176	2448
θ range for data collection[°]	2.71 to 26.31	3.89 to 69.97	2.92 to 62.21	3.73 to 69.91	1.66 to 26.33	1.73 to 27.45
Index ranges	$-12 \le h \le 17$ $-12 \le k \le 16$ $-16 \le l \le 16$	$-16 \le h \le 14$ $0 \le k \le 16$ $0 \le l \le 16$	$-21 \le h \le 0$ $0 \le k \le 8$ $-41 \le l \le 42$	$-17 \le h \le 15$ $0 \le k \le 15$ $0 \le l \le 17$	$-15 \le h \le 15$ $-9 \le k \le 18$ $-19 \le l \le 19$	$-21 \le h \le 22$ $-18 \le k \le 15$ $-29 \le l \le 25$
Refl. collected/unique [R_{int}]	5313/2565 [0.0307]	4439/4256 [0.0944]	8306/8033 [0.1566]	4833/4643 [0.0256]	20212/5776 [0.0576]	45537/12229 [0.0908]
Refl. observed ([$I_0 > 2\sigma(I_0)$])	2458	3935	3022	3905	4563	9290
Semi-emp. ψ-scan abs. corr.	Yes	Yes	Yes	Yes	No	No
Range of rel. transm. factors	1.019 and 0.982	2.390 to 0.713	1.707 to 0.791	1.264 to 0.861		
Data/restraints/parameters	2565/0/201	4256/0/292	8033/0/581	4643/0/286	5776/0/484	12229/0/589
Goodness-of-fit on F^2	1.139	1.044	1.018	1.031	1.037	1.024
SHELXL-97 wt. parameters	0.0321, 1.8277	0.096500, 2.563700	0.0647, 21.5658	0.069900, 2.340900	0.024000, 0.856200	0.080400, 0.000000
Final *R*1, *wR*2 [$I > 2\sigma(I)$]	0.0264, 0.0624	0.0476, 0.1311	0.0930, 0.1639	0.0417, 0.1108	0.0293, 0.0699	0.0460, 0.1182
*R*1, *wR*2 (all data)	0.0277, 0.0629	0.0502, 0.1340	0.2591, 0.2258	0.0506, 0.1171	0.0421, 0.0762	0.0634, 0.1292
Extinction Coefficient		0.0045(3)				
Diff. peak and hole (eÅ^{-3})	0.507 and –0.449	1.396 and –1.478	0.854 and –1.100	1.056 and –0.812	0.335 and –0.526	4.022 and –3.010

$L_{Me}Ir(COE)H_2$: The Ir-bound hydrides were not located. Crystal structure data for $L_{Me}Rh(COD)$, $L_{Me}Rh(C_2H_4)_2$, $L_{Cl}Rh(COE)$, $L_{Me}Rh(NBE)$, $L_{Me}Rh(COE)(MeCN)$, and $L_{Me}Ir(COE)H_2$; calculated total energies and atomic coordinates for the LRh and LIr complexes mentioned in the text. Crystallographic data (excluding structure factors) for the structures reported in this paper have been deposited with the Cambridge Crystallographic Data Centre as supplementary publication nos. CCDC-133849, CCDC-133850, CCDC-133851, CCDC-133852, CCDC-133853, and CCDC-133854. Copies of the data can be obtained free of charge on application to the CCDC, 12 Union Road, Cambridge CB2 1EZ, U.K. [Fax: (internat.) +44 (0)1223 336033; E-mail: deposit@ccdc.cam.ac.uk].

Acknowledgments

We are grateful to P. P. J. Schlebos (KUN) and H. Druijven (University of Groningen) for their able assistance in carrying out some of the NMR measurements. X-ray data for $L_{Me}Ir(COE)H_2$ and $L_{Me}Rh(COE)(MeCN)$ were collected on the CCD diffractometer of the national NWO-CW X-ray facility in Utrecht. Deuteration studies on 2,3-dimethyl-2-butene were carried out by H. van der Heijden and A. B. van Oort at the Shell Research and Technology Centre, Amsterdam. Bis(cyclohexylidene) was kindly provided by R. W. A. Havenith (University of Utrecht). We thank Johnson Matthey for a generous loan of rhodium and iridium chlorides.

[1] P. H. M. Budzelaar, A. B. van Oort, A. G. Orpen, *Eur. J. Inorg. Chem.* **1998**, 1485.

[2] For a preliminary account, see P. H. M. Budzelaar, R. de Gelder, A. W. Gal, *Organometallics* **1998**, *17*, 4122.

[3] Most of these complexes are chloro-bridged dimers in the solid state, but dissociate in solution. See, e.g. [3a] H. L. M. van Gaal, F. G. Moers, J. J. Steggerda, *J. Organomet. Chem.* **1974**, *65*, C43; H. L. M. van Gaal, F. L. A. van den Bekerom, J. P. J. Verlaan, *J. Organomet. Chem.* **1976**, *114*, C35; H. L. M. van Gaal, F. L. A. van den Bekerom, *J. Organomet. Chem.* **1977**, *134*, 237; C. Busetto, A. d'Alfonso, F. Maspero, G. Perego, A. Zazzetta, *J. Chem. Soc., Dalton Trans.* **1977**, 1828; P. R. Hoffman, T. Yoshida, T. Okano, S. Otsuka, J. A. Ibers, *Inorg. Chem.* **1976**, *15*, 2462; T. Yoshida, T. Okano, D. L. Thorn, T. H. Tulip, S. Otsuka, J. A. Ibers, *J. Organomet. Chem.* 1979, *181*, 183; P. Binger, J. Haas, G. Glaser, R. Goddard, C. Krüger, *Chem. Ber.* **1994**, *127*, 1927. – [3b] P. Hofmann, C. Meier, U. Englert, M. U. Schmidt, *Chem. Ber.* **1992**, *125*, 353.

[4] A. C. Cooper, W. E. Streib, O. Eisenstein, K. G. Caulton, *J. Am. Chem. Soc.* **1997**, *119*, 9069; A. C. Cooper, E. Clot, J. C. Huffman, W. E. Streib, F. Maseras, O. Eisenstein, K. G. Caulton, *J. Am. Chem. Soc.* **1999**, *121*, 97.

[5] J. M. Brown, P. J. Guiry, D. W. Price, M. B. Hursthouse, S. Karalulov, *Tetrahedron: Asymmetry* **1994**, *5*, 561.

[6] See, e.g. M. E. Howden, R. D. W. Kemmitt, M. D. Schilling, *J. Chem. Soc., Dalton Trans.* **1980**, 1716.

[7] A distorted T-shape and easy movement of the chlorine atom in three-coordinate bis(phosphane)RhCl complexes has been predicted on the basis of extended-Hückel calculations; see ref. [3b].

[8] The best data were obtained in [D_8]THF. Spectra in [D_8]THF, [D_{12}]cyclohexane (down to 6 °C), and [D_8]toluene (down to

–40 °C) were virtually identical, indicating the absence of significant THF coordination. However, the presence of some arene complexes (to be described in a future paper) in the toluene spectra made interpretation more difficult in these cases.

[9] The allyl hydride mechanism is one of the accepted mechanisms for olefin isomerization. However, only a few examples of rapid equilibration between the two structures have been reported: J. W. Byrne, H. U. Blaser, J. A. Osborn, *J. Am. Chem. Soc.* **1975**, *97*, 3871; H. Bönneman, *Angew. Chem.* **1970**, *82*, 699 (*Int. Ed. Engl.* **1970**, *9*, 736). Decomposition of rhodium(III) allyl hydride complexes to give free olefin has also been demonstrated: J. F. Nixon, B. Wilkins, *J. Organomet. Chem.* **1972**, *44*, C25; **1974**, *80*, 129. For an example of rapid allylic C–H activation at Ir, see R. Dorta, A. Togni, *Organometallics* **1998**, *17*, 5441.

[10] Reductive elimination from palladium(II) and platinum(II) allyl hydrides has been studied computationally: S. Sakaki, H. Satoh, H. Shono, Y. Ujino, *Organometallics* **1996**, *15*, 1713.

[11] The calculated energy difference between the olefin and allyl hydride is very sensitive to the method used. Hartree–Fock gives an even stronger preference for the olefin complex, while pure DFT[2] gives a smaller energy difference and a lower barrier. Apart from correlation treatment, sources of errors could be the basis set (not very large) and the lack of an explicit treatment of direct relativistic effects on the valence electrons.

[12] Steric effects are expected to favor the allyl hydride structure over the olefin complex because of the more "central" position of the allyl group relative to the diiminate aryl groups.

[13] Formation of iridium allyl hydrides from olefin precursors has been reported previously. See, e.g. R. S. Tanke, R. H. Crabtree, *Inorg. Chem.* **1989**, *28*, 3444; Y. Alvarado, O. Boutry, E. Gutiérrez, A. Monge, M. C. Nicasio, M. L. Poveda, P. J. Pérez, C. Ruiz, C. Bianchini, E. Carmona, *Chem. Eur. J.* **1997**, *3*, 860.

[14] The calculated energy difference between the Ir allyl hydride and olefin complexes is rather modest (6 kcal/mol; barrier 11 kcal/mol). If we assume that the 12 kcal/mol error in the case of Rh also applies to Ir, we would expect a preference in the "real" system of 18 kcal/mol and a barrier of 23 kcal/mol, which is compatible with the observed static room temperature spectrum. Unfortunately, L_{Me}Ir(H)(cyclooctenyl) decomposes rapidly on heating in solution, hence we could not verify the onset of dynamic behavior expected at higher temperatures.

[15] In addition to the signals of the dimethylbutene complex, some weak but sharp signals were observed, which could be attributed to the oxidation product L_{Me}Rh(OH)[η^3-$CH_2C(Me)CMe_2$] described in the section on hydrogenation.

[16] The Rh–H distance is calculated as 1.92 Å for a hydrogen placed at a calculated position with a standard C–H bond length of 0.97 Å. The actual C–H distance must be longer, as indicated by the low $^1J_{CH}$. However, the hydrogen atom position could not be refined satisfactorily.

[17] M. Pasquali, C. Floriani, A. Gaetani-Manfredotti, A. Chiesi-Villa, *J. Am. Chem. Soc.* **1978**, *100*, 4918.

[18] N. Carr, B. J. Dunne, L. Mole, A. G. Orpen, J. L. Spencer, *J. Chem. Soc., Dalton Trans.* **1991**, 863.

[19] M. Green, J. A. K. Howard, J. L. Spencer, F. G. A. Stone, *J. Chem. Soc., Dalton Trans.* **1977**, 171.

[20] D. D. LeCloux, S. J. Lippard, *Inorg. Chem.* **1997**, *36*, 4035.

[21] To assess the importance of the pre-organization of NBE, we also optimized the structures of two conformations of LRh(CPE) (CPE = cyclopentene). The CPE complex would be expected to have a weaker agostic interaction since it is less favorably pre-organized. On the other hand, if the interactions were strong, one would certainly expect to see a distortion here, whereas in the NBE complex the pre-organization might be so favorable that the agostic interaction would already be optimal in the undistorted structure. In fact, the energies of the "CH_2 in" and "CH_2 out" conformations of LRh(CPE) differ by less than 3 kcal/mol, and the RhH distance is long even in the "CH_2 in" conformation (2.58 Å; RhC = 2.98 Å; C–H = 1.104 and 1.093 Å). The angle between the $CH_2CH{=}CHCH_2$ plane and the Rh–olefin bond is nearly identical in the two conformations (97° for "CH_2 in", 98° for "CH_2 out"). These observations support our hypothesis that the agostic "bond" is not strong even in the NBE complex. The attractive force is rather weak, but since there is no *repulsive* force and the olefin is pre-organized, a close Rh–H contact still results.

[22] Because of the limited temperature region in which L_{Me}Rh(COE)(H_2) can be observed, T_1(min) studies were not carried out.

[23] See, e.g. R. H. Crabtree, *Acc. Chem. Res.* **1979**, *12*, 331.

[24] For a recent example of H/D exchange catalyzed by an Ir hydride, see E. Gutiérrez-Puebla, A. Monge, M. Paneque, M. L. Poveda, S. Taboada, M. Trujillo, E. Carmona, *J. Am. Chem. Soc.* **1999**, *121*, 346.

[25] See, e.g. B. Moreno, S. Sabo-Etienne, B. Chaudret, A. Rodriguez, F. Jalon, S. Trofimenko, *J. Am. Chem. Soc.* 1995, *117*, 7441; M. T. Bautista, E. P. Cappellani, S. D. Drouin, R. H. Morris, C. T. Schweitzer, A. Sella, J. Zubkowski, *J. Am. Chem. Soc.* **1991**, *113*, 4876 and references cited therein.

[26] The presence of small amounts of a COD isomer (GC/MS) in the COE could be detected by GC. It differed from authentic samples of 1,3-COD and 1,5-COD and so was most likely 1,4-COD. Identification of the deactivation product as a 1,4-COD complex was achieved by comparison with pure L_xRh(1,4-COD) prepared from L_xRh(COE) and 1,3-COD; see details in Experimental Section.

[27] Oxidative addition of aromatic C–halogen bonds will be reported separately.

[28] B. James, *Addition of Hydrogen and Hydrogen Cyanide to Carbon–Carbon Double and Triple Bonds*, in *Comprehensive Organometallic Chemistry* (Ed.: G. Wilkinson), Pergamon, Oxford, **1982**, vol. 8, p 285–369. See also P. A. Chaloner, M. A. Esteruelas, F. Joó, L. A. Oro, *Homogeneous Hydrogenation*, Kluwer, Dordrecht, **1994**.

[29] See, e.g. J. Halpern, D. P. Riley, A. S. C. Chan, J. J. Pluth, *J. Am. Chem. Soc.* **1977**, *99*, 8055; A. S. C. Chan, J. J. Pluth, J. Halpern, *J. Am. Chem. Soc.* **1980**, *102*, 5952; C. R. Landis, J. Halpern, *J. Organomet. Chem.* 1983, *250*, 485; C. R. Landis, J. Halpern, *J. Am. Chem. Soc.* **1987**, *109*, 1746.

[30] In the Wilkinson system, phosphane recoordination is believed to precede alkane elimination (ref.[31]).

[31] See, e.g. J. Halpern, C. S. Wong, *J. Chem. Soc., Chem. Commun.* **1973**, 629; J. Halpern, in *Organotransition Metal Chemistry* (Eds.: Y. Ishii, M. Tsutsui), Plenum, New York, **1975**, p. 109; J. Halpern, T. Okamoto, A. Zakhariev, *J. Mol. Catal.* **1976**, *2*, 65. For theoretical studies, see e.g. A. Dedieu, *Inorg. Chem.* **1980**, *19*, 375; C. Daniel, N. Koga, J. Han, X. Y. Fu, K. Morokuma, *J. Am. Chem. Soc.* **1988**, *110*, 3773.

[32] We have also briefly investigated complexes of related ligands bearing 2,4,6-$Me_3C_6H_2$ and 2,6-(iPr)$_2C_6H_3$ groups at N. The chemistry appears to be similar, but many complexes were obtained as oils and could not be purified.

[33] See, e.g. C. P. Casey, E. L. Paulsen, E. W. Beuttenmueller, B. R. Proft, B. A. Matter, D. R. Powell, *J. Am. Chem. Soc.* **1999**, *121*, 63.

[34] All calculations were carried out with the Gaussian program (*Gaussian 94*, *Revision E.1*, M. J. Frisch, G. W. Trucks, H. B. Schlegel, P. M. W. Gill, B. G. Johnson, M. A. Robb, J. R. Cheeseman, T. Keith, G. A. Petersson, J. A. Montgomery, K. Raghavachari, M. A. Al-Laham, V. G. Zakrzewski, J. V. Ortiz, J. B. Foresman, J. Cioslowski, B. B. Stefanov, A. Nanayakkara, M. Challacombe, C. Y. Peng, P. Y. Ayala, W. Chen, M. W. Wong, J. L. Andres, E. S. Replogle, R. Gomperts, R. L. Martin, D. J. Fox, J. S. Binkley, D. J. Defrees, J. Baker, J. P. Stewart, M. Head-Gordon, C. Gonzalez, J. A. Pople, Gaussian, Inc., Pittsburgh PA, **1995**.

[35] S. Binkley, J. A. Pople, W. J. Hehre, *J. Am. Chem. Soc.* **1980**, *102*, 939.

[36] P. J. Hay, W. R. Wadt, *J. Chem. Phys.* **1985**, *82*, 299.

[37] A. D. Becke, *J. Chem. Phys.* **1993**, *98*, 5648.

[38] G. Giordano, R. H. Crabtree, *Inorg. Synth.* **1990**, *28*, 88.

[39] R. Cramer, *Inorg. Synth.* **1990**, *28*, 86.

[40] A. van der Ent, A. L. Onderdelinden, *Inorg. Synth.* **1990**, *28*, 90.

[41] A. C. T. North, D. C. Philips, F. S. Mathews, *Acta Crystallogr.* **1968**, *A24*, 351.

[42] P. T. Beurskens, G. Beurskens, M. Strumpel, C. E. Nordman, in "Patterson and Pattersons" (Eds.: J. P. Glusker, B. K. Patterson, M. Rossi), Clarendon Press, Oxford, **1987**, p. 356.

[43] P. T. Beurskens, G. Beurskens, W. P. Bosman, R. de Gelder, S. Garcia-Granda, R. O. Gould, R. Israel, J. M. M. Smits, *DIRDIF-96*: A computer program system for crystal structure determination by Patterson methods and direct methods ap-

plied to difference structure factors, Crystallography Laboratory, University of Nijmegen, The Netherlands, **1996**.
[44] G. M. Sheldrick, *SHELXL-97: Program for the refinement of crystal structures*, University of Göttingen, Germany, **1997.**
[45] A. L. Spek, *Acta Crystallogr.* **1990**, *A46*, C34; A. L. Spek, *PLATON-93*: *Program for display and analysis of crystal and molecular structures*, University of Utrecht, The Netherlands, **1995**.

Received September 16, 1999
[I99328]